COMPETITION BETWEEN CHAOS CONTROL AND CHAOS SYNCHRONIZATION IN SMALL SIZED NETWORKS

by

Özgür Aktekin

B.S., Control Engineering, Istanbul Technical University, 2010

Submitted to the Institute for Graduate Studies in
Science and Engineering in partial fulfillment of
the requirements for the degree of
Master of Science

Graduate Program in Electrical and Electronics Engineering
Boğaziçi University
2017

ACKNOWLEDGEMENTS

I would like to offer my deep and sincere gratitude to Prof. Dr. Yağmur Denizhan for her precious advice, guidance and the continuing support she has shown throughout this research, and throughout my study at Boğaziçi University. Without her encouragements, her enthusiasm, and her unselfish help, I could never finish my master work. She has spent countless hours working with me and has inspired and motivated me to finish on time.

I am also thankful to the members of thesis evaluation committee, Prof. Dr. Neslihan Serap Şengör and Asst. Prof. Dr. Janset Daşdemir. Their comments and suggestions have enhanced the quality of my thesis.

I am also thankful to my lifelong friends, Ali Onur, Selim, İsmail, Burcu, Hüseyin, Alican and Uğur for all the helpful discussions that I had with them over the years. My gratitude also goes to all the staffs of AVL Turkey.

I owe a huge debt of gratitude to my mother and my sister for being very supportive of all my decisions in my life. They have always put my needs ahead of theirs.

Last but not least, I am greatly indebted to my father for being supportive for freely thinking and providing a vision for my academic career. He is my inspiration for good work, ethics and diligence.

To my father...

ABSTRACT

COMPETITION BETWEEN CHAOS CONTROL AND CHAOS SYNCHRONIZATION IN SMALL SIZED NETWORKS

Control and synchronization of chaotic systems have been two important issues of investigation in the field of chaotic dynamics since early 1990s. Stabilization of chaotic systems at an unstable periodic orbit (UPO) via small parameter perturbations using local linear feedback proposed by Ott, Grebogi and Yorke (OGY method) is one of the earliest and best known techniques for chaos control and has numerous applications, modifications and extensions in the literature. On the other hand, synchronizability of coupled chaotic systems, which exhibit the so called decomposability property, has been demonstrated by Pecora and Carroll (PC-decomposition) in 1990, and has paved the way for diverse studies and applications of chaos synchronization using different configurations and coupling schemes ever since.

In this thesis, an original investigation is conducted where a small number of identical chaotic systems stabilized at distinct UPOs by a modified version of the OGY method are coupled according to a selective coupling strategy such that the two tendencies, i. e. the tendency of each system to follow its own distinct UPO and the tendency of the coupled systems to synchronize, compete. It is also studied how this competition can be influenced by an external static disturbance that effects all systems in the same manner.

ÖZET

KÜÇÜK BOYUTLU AĞLARDA KAOS KONTROLÜ VE KAOS SENKRONİZASYONU ARASINDA REKABET

Kaotik sistemlerin kontrolü ve senkronizasyonu 1990'ların başından bu yana kaotik dinamik alanında iki önemli araştırma konusu oldular. Küçük parametre değişiklikleri yaparak kaotik bir sistemi kararsız bir yörünge üzerinde kararlı kılan OGY yöntemi, Ott, Grebogi ve Yorke tarafından önerilmiş olup, en eski ve en tanınmış kaos kontrol yöntemlerinden biridir. Literatürde bu yöntemin çok sayıda uygulama, uyarlama ve uzantıları bulunmaktadır. Öte yandan, dekompoze edilebilirlik özelliğine sahip kuple edilmiş kaotik sistemlerin senkronize olabildiği Pecora ve Carroll tarafından 1990 yılında gösterilmiş, böylece daha sonra yapılan ve farklı kurulum ve kuplaj şemaları kullanan çeşitli kaos senkronizasyonu araştırma ve uygulamalarına öncülük etmiştir.

Bu tezde yapılan özgün araştırmada, uyarlanmış bir OGY yöntemiyle farklı kararsız periyodik yörünge üzerinde kararlı hale getirilmiş bir kaç özdeş kaotik sistem, seçici bir kuplaj stratejisine göre kuple edilmiş, böylece her bir sistemin kendi periyodik yörüngelerini izleme eğilimiyle, kuple olmuş sistemlerin senkronize olma eğiliminin rekabet etmesi sağlanmıştır. Ayrıca tüm sistemleri aynı şekilde etkileyen dışsal statik bir bozucunun bu rekabeti nasıl etkilediği incelenmiştir.

TABLE OF CONTENTS

ACKNOWLEDGEMENTS iii
ABSTRACT v
ÖZET vi
LIST OF FIGURES ix
LIST OF TABLES xii
LIST OF SYMBOLS xiii
LIST OF ACRONYMS/ABBREVIATIONS xv
1. INTRODUCTION 1
2. THEORETICAL FOUNDATION 5
2.1. Dynamical Systems 5
2.2. Synchronization 12
2.2.1. Some Common μ-Functions for Coupling Two Systems 13
2.2.1.1. Weighted Average of Full-State Vectors 14
2.2.1.2. Weighted Average of a Subset of States 14
2.2.1.3. Difference of Full-State Vectors 15
2.2.1.4. Difference of a Subset of States 15
2.2.2. Some Common F-Functions for Coupling Two Systems 15
2.2.2.1. Replacement of a Subset of States 15
2.2.2.2. Additive Linear Coupling 16
2.3. Synchronization of Two Oscillators 16
2.4. Decomposition Based Synchronization of Coupled Chaotic Systems . . 17
2.5. Chaos Control via OGY Method 20
3. INVESTIGATION OF DIFFERENT COUPLING CONFIGURATIONS FOR DECOMPOSITION BASED CHAOS SYNCHRONIZATION 27
3.1. Considered Coupling Configurations 28
3.2. Selected Coupling Configuration 33
4. PREPARATIONS FOR COMBINING OGY CONTROL AND DECOMPOSITION BASED SYNCHRONIZATION 34
4.1. Control-Saturated OGY Control (CS-OGY) 34

4.2. Selective Coupling Strategy 37
5. CS-OGY COMBINED WITH DECOMPOSITION BASED SYNCHRONIZATION 43
5.1. Different Regimes for Two Chaotic Systems 44
5.1.1. Nonsynchronized Chaotic Motion 44
5.1.2. Synchronized Chaotic Motion 44
5.1.3. Chaotic and Periodic Motions 45
5.1.4. Independent Periodic Motion 45
5.2. The Effect of Disturbance 46
5.3. Multi-Node Networks 47
6. CONCLUSION 52
6.1. Novel Synchronization Scheme 52
6.2. Novel Modification of the OGY Method 53
6.3. Control-Similarity Based Coupling 53
6.4. Competition between Control and Synchronization 54
6.5. Effect of Common Disturbance 54
6.6. Conclusion 55
REFERENCES 56
APPENDIX A: STABILITY DEFINITIONS 64
APPENDIX B: DEFINITIONS OF SYNCHRONIZATION 67
APPENDIX C: CS-OGY ALGORITHM 69
APPENDIX D: PROOF OF THE STABILITY OF THE SYNCHRONIZATION OF BI-DIR-AD MEAN-FIELD COUPLED LORENZ SYSTEMS 70

LIST OF FIGURES

Figure 2.1. Periodic orbit 7

Figure 2.2. Poincaré surface of section for 3D space 10

Figure 2.3. Strange attractors 12

Figure 2.4. Sample Coupling Configurations of Networks 13

Figure 2.5. Decomposition-based master-slave coupling 18

Figure 2.6. Synchronization of two Lorenz systems which are master-slave coupled using the x-state as the drive component 19

Figure 2.7. OGY control of the Logistic map with $a_{nom} = 3.9$, and the target $x^* = 0.745$, $\Delta a = 0.001$ and $R_{OGY} = 0.001$ 24

Figure 2.8. OGY control of the Logistic map with $a_{nom} = 3.9$, and the target $x^* = 0.745$, $\Delta a = 0.1$ and $R_{OGY} = 0.01$ 25

Figure 2.9. OGY Control of the Henon map with $(a_{nom}, b_{nom}) = (1.37, 0.3)$, and target $\mathbf{w}^* = [0.877, 0.877]^\top$, $\Delta a = 0.03$ and $R_{OGY} = 0.2$ 26

Figure 3.1. Four possible coupling configurations 28

Figure 3.2. States of two uni-dir-AD coupled systems (D_1 master, D_2 slave). . 31

Figure 3.3. States of two uni-dir-CD coupled systems (D_1 master, D_2 slave). . 31

Figure 3.4. States of two bi-dir-AD coupled systems. 32

Figure 3.5. States of two bi-dir-CD coupled systems. 32

Figure 4.1. CS-OGY sections of the Lorenz attractor for different initial conditions 35

Figure 4.2. States and control parameter variations of a Logistic map with $a_{nom} = 1.37$ stabilized at $x^* = 0.744$ by (a) basic OGY with $R_{OGY} = 0.01$, and (b) CS-OGY with $\mid \Delta a \mid < 0.1$ 36

Figure 4.3. States and control parameter variations of a Henon map with $(a_{nom}, b_{nom}) = (1.37,\ 0.3)$ stabilized at $\mathbf{w}^* = [0.877, 0.877]^\top$ by (a)basic OGY with $R_{\mathrm{OGY}}{=}0.2$, and (b)CS-OGY with $|\Delta a|{<}0.03$. 36

Figure 4.4. Stabilized UPOs of the Lorenz system 40

Figure 4.5. The control inputs (u_1, u_2) and the coupling statuses $(\gamma_{12}, \gamma_{21})$ of two CS-OGY controlled systems stabilized at UPO_1 and UPO_2 under CoSim-based coupling with $\alpha = 1$, $\nu = 0.5$, $\theta_{CoSim} = \delta \times 10^{-3}$ and (a) $\kappa = 3$, (b) $\kappa = 20$ 41

Figure 4.6. The control inputs (u_1, u_2) and the coupling statuses $(\gamma_{12}, \gamma_{21})$ of two CS-OGY controlled systems stabilized at UPO_1 and UPO_2 under CoSim-based coupling with $\kappa = 5$, $\nu = 0.5$ $\theta_{CoSim} = \delta \times 10^{-3}$ and (a) $\alpha = 1$, (b) $\alpha = 0.3$ 41

Figure 4.7. The control inputs (u_1, u_2) and the coupling statuses $(\gamma_{12}, \gamma_{21})$ of two CS-OGY controlled systems stabilized at UPO_1 and UPO_2 under CoSim-based coupling with $\kappa = 6$, $\alpha = 0.7$, $\theta_{CoSim} = \delta \times 10^{-3}$ and (a) $\nu = 0.5$, (b) $\nu = 0.9$ 42

Figure 4.8. The control inputs (u_1, u_2) and the coupling statuses (γ_{12}, γ_{21}) of two CS-OGY controlled systems stabilized at UPO_1 and UPO_2 under CoSim-based coupling with $\kappa = 6$, $\alpha = 0.7$, $\nu = 0.9$ and (a) $\theta_{CoSim} = 0.001 \times \delta$ (b), $\theta_{CoSim} = 0.5 \times \delta$ 42

Figure 5.1. Different regimes for two identical chaotic systems under CoSim-based coupling CS-OGY control with distinct target UPOs 45

Figure 5.2. Transitions between different regimes in a two-node network consisting of two chaotic systems under CoSim-based coupling and CS-OGY control with target UPO_1 and UPO_2 respectively. 48

Figure 5.3. Effect of common disturbance in a two node network (β is increased from 8/3 to 3 at 175 sec.) 49

Figure 5.4. Transitions between different regimes in a three-node network consisting of three chaotic systems under CoSim-based coupling and CS-OGY control with target UPO_1, UPO_2 and UPO_3 respectively. 50

Figure 5.5. Transitions between different regimes in a four-node network consisting of four chaotic systems under CoSim-based coupling and CS-OGY control with target UPO_1, UPO_2, UPO_3 and UPO_1 respectively. 51

Figure C.1. CSS-OGY Control Algorithm 69

LIST OF TABLES

Table 3.1. Synchronization ranges for investigated coupling configurations . . 30

Table 4.1. Characteristics of the target UPOs of used in the simulations . . . 39

LIST OF SYMBOLS

$\mathbf{A}$	State matrix
$\mathbf{B}$	Input matrix
$\mathbf{C}$	Control similarity matrix
E	Energy function
$\mathbf{K}$	Control matrix
n	dimension of a system
N	number of elements in a Network
$\mathbf{P}$	Poincaré map
R_{OGY}	OGY radius
S_p	Poincaré surface of section
T	Period of an oscillator
T_s	Sampling period
u	Input of a system
V	Lyapunov function
$\mathbf{w}$	State of a continuous time system
α	Forgetting factor
β	Parameter of the Lorenz System
δ_i	Maximum allowed parameter change for OGY method
Δs	Thickness for Poincaré intersection detection
Δp	Parameter perturbation for OGY method
ϵ	Coupling influence coefficient
Φ	Transformation matrix
γ_{ij}	Coupling of i^{th} element to j^{th} element in the system
$\mathbf{\Gamma}$	Coupling matrix
$\boldsymbol{\eta}$	State of a discrete-time system for OGY method
κ	Memory span
λ	Lyapunov exponent

μ	Coupling variable
ν	Similarity ratio threshold
θ_{CoSim}	Control similarity threshold
ρ	Parameter of the Lorenz System
σ	Parameter of the Lorenz System
τ	Time shift
Ω_{OGY}	OGY region
ψ	Projection scalar
$\boldsymbol{\zeta}$	State of a discrete-time system

LIST OF ACRONYMS/ABBREVIATIONS

2D	Two Dimensional
3D	Three Dimensional
bi-dir-AD	Bidirectional autonomous coupling architecture
bi-dir-CD	Bidirectional coupled coupling architecture
CoSim	Control Similarity
CS	Complete Synchronization
CS-OGY	Control-Saturated OGY Control
DLQR	Discrete Linear Quadratic Regulator
FPrS	Function Projective Synchronization
GS	Generalized Synchronization
IC	Initial Condition
LS	Lag Synchronization
MFPrS	Modified Function Projective Synchronization
OGY	Ott-Grebogi-Yorke
PhS	Phase Synchronization
PrLS	Projective Lag Synchronization
PrS	Projective Synchronization
UEP	Unstable Equilibrium Point
uni-dir-AD	Unidirectional autonomous coupling architecture
uni-dir-CD	Unidirectional autonomous coupling architecture
UPO	Unstable Periodic Orbit

1. INTRODUCTION

Chaos is a commonly observable phenomenon in nature. Studies of dynamical systems which are capable of exhibiting a dynamic behavior, which has later been called deterministic chaos, go back to the 19^{th} century when Henri Poincaré worked on the three body problem. Many natural systems from meteorology to biology exhibit chaotic behavior. Deterministic chaos has become a widely investigated topic since Ed Lorenz published in 1963 his paper on the nonperiodic dynamics of atmospheric convection [1]. After the work of Li and Yorke in 1973 [2], which was the first time the word *chaos* was used in the scientific literature, the number of articles published increased rapidly and chaos has become an emerging topic in mathematics. A general characteristic of deterministic chaotic dynamics is long-term unpredictability, which is a result of high sensitivity to initial conditions. Lorenz simply defines deterministic chaotic systems as systems, for which the current state determines the future state, however, approximation of the current state does not determine the approximate future state. Chaotic systems are highly sensitive to initial conditions, observation errors, measurement noise, and parameter changes.

In addition to Lorenz's convection model, various chaotic mathematical benchmark models have been proposed in the literature, such as; the Logistic equation [3], the Henon map [4], the Rössler system [5] and Chua's circuit [6].

As Chaos Theory became a significant area of research, many related new issues emerged. Investigations on the control of chaotic systems and synchronization of coupled chaotic systems are among them.

Control of chaos first arose in the literature with the idea of forcing a chaotic system in a periodic manner. In 1990, Ott, Grebogi and Yorke proposed a method to control chaotic systems by stabilizing one of the infinitely many unstable periodic orbits (UPOs) of the chaotic system via small parameter perturbations using feedback control. This method has later been named OGY control [7]. OGY control uses some basic attributes of dissipative chaotic systems which have strange attractors. Typically, such a strange attractor harbors infinitely many embedded UPOs. One of them is first chosen as the target UPO. When the system passes through a close neighborhood of the chosen UPO, some of the system parameters can be slightly varied in order to stabilize this UPO. In order to achieve this, a local linear model of the system in the close neighborhood of the target UPO has to be obtained from empirical data. A linear controller based on this empirical model is activated when the system enters the close neighborhood of the target UPO and stabilizes it, such that the system remains trapped in it. Various applications [8–11] and extensions [12–18] of the OGY control method exist in the literature. The particular type of chaos control that will be used in this thesis is a slightly modified version of the original OGY control.

In addition to the stabilization of a chaotic system on a UPO or at an unstable equilibrium point (UEP) of the system itself, stabilization on an externally imposed reference trajectory or a reference point, and synchronization with another system can be mentioned among approaches to chaos control. In 1992, Pyragas proposed the Delayed Feedback method which is based on a continuous feedback law for stabilizing periodic orbits [19]. Further extensions of delayed feedback methods to coupled systems [20] and discrete-time systems also exist in the literature [21, 22]. Besides, classical control methods are applied to chaotic systems. Adaptive control method is used to stabilize a chaotic system at a reference point [23,24], to achieve synchronization of two chaotic oscillators [25–28], or to stabilize the system at one of its embedded UPOs [29]. Moreover, due to the highly nonlinear nature of chaotic systems fuzzy control [30–33], and neural network based control methods [34,35] are also considered and successfully applied.

Synchronization is a phenomenon where two or more oscillators arrange a feature or features of their oscillation (such as frequency or phase) according to an external force or some interaction between each other. As commonly observable examples of synchronization, applauding audience in a theater, a group of soldiers marching, bird or fish swarms, or flashing fire flies can be mentioned. Synchronization in dynamical systems has attracted wide interest for centuries since the Dutch scientist Christian

Huygens observed how pendulum clocks hanging on the same a wall tend to synchronize. In some cases, synchronization is a goal that systems have to achieve as the case in communication, music or lasers. On the other hand, in some other systems such as vibration of bridges or buildings, it is a phenomenon to be avoided because of its highly destructive capacity.

As chaos theory is studied widely, synchronization of a class of chaotic systems under certain coupling conditions became of interest. In 1990, in parallel to the first chaos control studies, Pecora and Carroll published their article on synchronization of chaotic oscillators and showed the possibility of synchronizing a chaotic system to another identical system, which drives the former by direct state replacement [36]. In 1993, Cuomo and Oppenheim [37] designed an electronic circuit based on Pecora and Carroll's work to demonstrate application of synchronization of chaotic systems in secure communication. Following Pecora and Carroll's work, numerous studies with various coupling configurations and synchronization definitions are published on synchronization of identical [38–40] and nonidentical chaotic systems [41–43]. In addition to these studies, others which consider a network of coupled systems and different coupling configurations among them takes an important place in the field of synchronization of chaotic oscillators [44–47].

In this thesis, an original investigation is conducted on how control and synchronization of chaotic systems can be combined and how they would interfere with each other if the systems are coupled according to a special coupling scenario. For that purpose, a small number of identical chaotic systems have been considered, which are stabilized by a modified version of OGY method at distinct UPOs. This modification is dubbed control-saturated OGY control (CS-OGY). The coupling is established according to a novel selective coupling strategy such that the two tendencies, - namely the tendency of each system to follow its own distinct UPO and the tendency of the coupled systems to move on the strange attractor in a synchronized manner - can compete with each other. It has been also studied how this competition is influenced by an external static disturbance that affects all involved systems in the same manner.

The thesis is organized as follows: In Section II, the fundamental notions related to dynamical systems and deterministic chaotic systems are defined. The synchronization phenomenon is explained in detail, and coupling configurations and coupling schemes are described. Chaos synchronization and different methods of achieving it are explained. Additionally, the basic OGY control method is introduced along with its extensions and some examples.

In Section III, investigations on alternative coupling configurations are presented with the numerical simulations, and the chosen one to be used in the rest of the thesis is provided.

Problem statement is given in Section IV. Also, a slightly modified OGY control algorithm, which is named control-saturated OGY (CS-OGY), is presented. Moreover, a selective coupling strategy is introduced, which is based on the similarity of the control actions of the involved systems.

In the fifth section, possible scenarios, which can be observed during the competition between, control and synchronization are explained. Numerical simulations are performed on the Lorenz system for networks of two, three and four nodes.

In the sixth section, concluding remarks on the novel synchronization scheme, CS-OGY method, selective coupling strategy, competition between synchronization and control and the effect of common disturbance are given. Finally, some research directions are proposed for future investigations.

2. THEORETICAL FOUNDATION

2.1. Dynamical Systems

In mathematics and engineering dynamical systems are represented in terms of mathematical models which describe the temporal evolution of the system states. Systems that have to be represented by models involving randomness are called *stochastic systems*. In *stochastic systems*, different outputs can be generated for the same initial conditions and system parameters. On the other hand, dynamical systems, for which the states evolve in a unique manner, determined by the initial conditions and system parameters, are called *deterministic systems*.

In this thesis, only deterministic systems are considered, which lend themselves to a representation in terms of either ordinary differential equations or ordinary difference equations. More specifically, *continuous time systems* are represented by differential equations, while *discrete-time systems* are represented by difference equations. Here, only *continuous time systems* will be considered, which can be represented in the general form

$$\dot{\mathbf{w}}(t) = \mathbf{f}(\mathbf{w}(t), \mathbf{u}(t)) \tag{2.1}$$

where $\mathbf{w}(t) = [w_1(t), w_2(t), ..., w_n(t)]^\top \in \mathbf{R}^n$ and $\mathbf{u}(t) = [u_1(t), u_2(t), ..., u_m(t)]^\top \in \mathbf{R}^m$ are the state and the input vectors, respectively, and $\mathbf{f}$ is an n-dimensional vector function called the *system function*.

Similarly, only *discrete time dynamical systems* will be considered, which are representable as

$$\boldsymbol{\zeta}(k+1) = \mathbf{g}(\boldsymbol{\zeta}(k), \mathbf{u}(k)) \tag{2.2}$$

where $\boldsymbol{\zeta}(k) = [\zeta_1(k), \zeta_2(k), ..., \zeta_n(k)]^\top \in \mathbf{R}^n$ is the state vector of the n-dimensional dynamical system, $\mathbf{u}(k) = [u_1(k), u_2(k), ..., u_m(k)]^\top \in \mathbf{R}^m$ is the input vector and $\mathbf{g}$ is an n-dimensional vector function called the *system function.*

Linear systems constitute a special case of the general nonlinear systems of the form Equation 2.1 or 2.2, where the system functions $\mathbf{f}$ or $\mathbf{g}$ are linear in the state and input variables Thus, continuous-time linear dynamical systems can be represented as

$$\dot{\mathbf{w}}(t) = \mathbf{A}\mathbf{w}(t) + \mathbf{B}\mathbf{u}(t) \tag{2.3}$$

while discrete-time linear systems can be represented as

$$\boldsymbol{\zeta}(k+1) = \mathbf{A}\boldsymbol{\zeta}(k) + \mathbf{B}\mathbf{u}(k) \tag{2.4}$$

where $\mathbf{A}$ is an $n \times n$ matrix and $\mathbf{B}$ is an $n \times m$ matrix, $\mathbf{w}(t)$, $\boldsymbol{\zeta}(k) \in \mathbf{R}^n$ represent the state vectors and $\mathbf{u}(t)$, $\mathbf{u}(k) \in \mathbf{R}^m$ represent the input vectors, respectively.

An *equilibrium behavior* of a dynamical system is a behavior, which is sustained in complete absence of perturbations. *Equilibrium behaviors* can be subdivided into static and dynamic ones. Static equilibrium behavior corresponds to the resting behavior at an equilibrium point, while dynamic equilibrium behaviors include periodic motion on a closed orbit and the motion on a chaotic attractor. An *equilibrium point*, $\mathbf{w}^*$, of a continuous dynamical system of the form given in Equation 2.1 has to satisfy Equation 2.5 and the equilibrium point $\boldsymbol{\zeta}^*$ of a discrete-time dynamical system of the form given in Equation 2.2 has to satisfy Equation 2.6.

$$\dot{\mathbf{w}}(t) = \mathbf{f}(\mathbf{w}(t)) = \mathbf{f}(\mathbf{w}^*) = \mathbf{0} \tag{2.5}$$

$$\boldsymbol{\zeta}(k+1) = \mathbf{f}(\boldsymbol{\zeta}(k)) = \boldsymbol{\zeta}^* \tag{2.6}$$

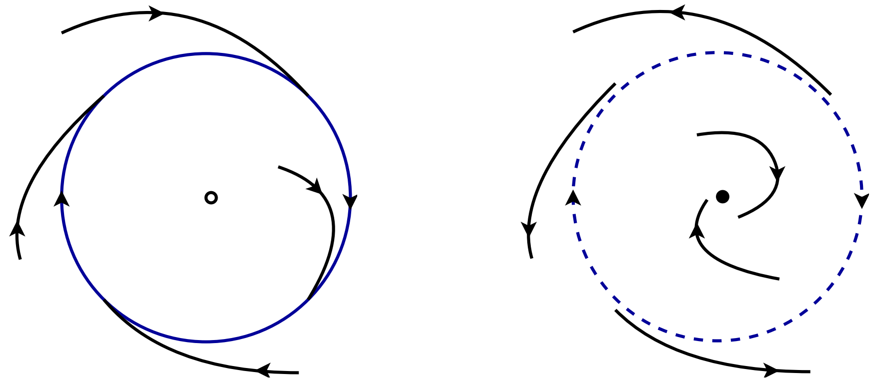

(a) Stable periodic orbit (b) Unstable periodic orbit

Figure 2.1. Periodic orbit

A periodic orbit is a system behavior, where the system state repeats itself with a period T. A period-T periodic orbit, $\mathbf{w}^*(t)$, of a continuous time system has to satisfy Equation 2.7, while the periodic points, $\boldsymbol{\zeta}_i^*$ that constitute a period T-cycle of a discrete-time system have to satisfy Equation 2.8.

$$\mathbf{w}(t) = \mathbf{w}(t+T) = \mathbf{w}^*(t) \tag{2.7}$$

$$\boldsymbol{\zeta}(k) = \boldsymbol{\zeta}(k+T) = \boldsymbol{\zeta^*}_i \quad i = 1, \ldots, T \tag{2.8}$$

For discrete time systems, a period-1 point, $\boldsymbol{\zeta}^{*1}$, is same thing as an equilibrium point, $\boldsymbol{\zeta}^*$, and it is also referred to as the *period-1* orbit of the system.

An important issue related to equilibrium behaviors is whether they are stable. In its most general sense, the stability of an equilibrium behavior implies that the system states which are very close to that behavior will remain close for all times. The stricter notion of asymptotic stability requires that system trajectories starting close to an equilibrium behavior asymptotically converge to it. More detailed definitions of stability are given in Appendix A.

Equilibrium behaviors that are asymptotically stable are called *attractors*. Thus, depending on the type of the equilibrium behavior, there exist basically three different attractor categories: *point attractor* (an asymptotically stable equilibrium point), *periodic attractor* (an asymptotically stable periodic orbit) and *strange (or chaotic) attractor* (the part of the state space occupied by the steady state behavior of a dissipative chaotic system, typically having fractal dimensions).

If the neighborhood of an equilibrium point or periodic orbit within which the stability conditions are valid, contains the whole state space, the stability is said to be global, otherwise it is local. If a system has an attractor (asymptotically stable equilibrium point, asymptotically stable periodic orbit or strange attractor), the set of initial conditions, starting from which the system converges to the attractor, is called the *basin of attraction* of that attractor. For linear systems and globally stable nonlinear systems, *basin of attraction* is the whole state space by definition.

Nonlinear dynamical systems representable in the form of Equation 2.1 can be locally approximated by a linear model in a close neighborhood of an equilibrium point, $\mathbf{w}^*$, and for inputs that are close enough to a nominal input value, $\mathbf{u_{nom}}$, if the system function $\mathbf{f}$ is differentiable and its Jacobian ($\mathbf{J}$) is non-singular at $\mathbf{w}^*$ and $\mathbf{u_{nom}}$.

$$\mathbf{A_{lin}} = \frac{\partial \mathbf{f}(\mathbf{w}(t), \mathbf{u}(t))}{\partial \mathbf{w}(t)}|_{(\mathbf{w}^*, \mathbf{u_{nom}})} = \begin{bmatrix} \frac{\partial f_{w_1}}{\partial w_1} & \cdots & \frac{\partial f_{w_1}}{\partial w_n} \\ \vdots & \ddots & \vdots \\ \frac{\partial f_{w_n}}{\partial w_1} & \cdots & \frac{\partial f_{w_n}}{\partial w_n} \end{bmatrix}_{(\mathbf{w}^*, \mathbf{u_{nom}})} \tag{2.9}$$

and for input matrix

$$\mathbf{B_{lin}} = \frac{\partial \mathbf{f}(\mathbf{w}(t), \mathbf{u}(t))}{\partial \mathbf{u}(t)}|_{(\mathbf{w}^*, \mathbf{u_{nom}})} = \begin{bmatrix} \frac{\partial f_{w_1}}{\partial u_1} & \cdots & \frac{\partial f_{w_1}}{\partial u_m} \\ \vdots & \ddots & \vdots \\ \frac{\partial f_{w_n}}{\partial u_1} & \cdots & \frac{\partial f_{w_n}}{\partial u_m} \end{bmatrix}_{(\mathbf{w}^*, \mathbf{u_{nom}})} \tag{2.10}$$

Nonlinear dynamical systems typically have a rich dynamic repertoire. A small variation in a parameter value of such system can result in a qualitative change in the system behavior, which may be associated with the birth or destruction of equilibrium points or periodic orbits, or with a change of their stability. Such a qualitative change in the dynamic behavior as a result of infinitesimal parameter change is called a *bifurcation*.

Although equilibrium points can be relatively easily calculated from the system equations, periodic orbits of continuous-time systems cannot be analytically found in general. To detect and analyze periodic orbits of continuous-time systems, one can make use of the so-called *Poincaré section* method. Consider an n dimensional dynamical system in the form of Equation 2.1. Place an $n-1$ dimensional hyper surface transverse to vector field $\mathbf{f}(\mathbf{w}(t))$ and specify a direction of traversal with it. This hyper surface is called a Poincaré surface, $\mathbf{S}_p$. Swirling system trajectories can pierce $\mathbf{S}_p$ in the specified direction more than once. The map that associates successive piercing points, $\boldsymbol{\zeta}(k)$ and $\boldsymbol{\zeta}(k+1)$, is called the Poincaré map, $\mathbf{P}(\boldsymbol{\zeta}(k))$, associated with $\mathbf{S}_p$. A *Poincaré map* of an n-dimensional continuous-time system of the form Equation 2.1 is defined as

$$\boldsymbol{\zeta}(k+1) = \mathbf{P}(\boldsymbol{\zeta}(k)) \tag{2.11}$$

where $\boldsymbol{\zeta}(k) \in \mathbf{S}_p$ is the point where the system trajectory pierces $\mathbf{S}_p$ in the specified direction for the k^{th} time. Since all piercing points have to be on $\mathbf{S}_p$, one dimension of the map can be discarded, reducing it to an $(n-1)$-dimensional map without loss of information.

It should be noted that a periodic orbit of the continuous-time system which transverses $\mathbf{S}_p$ in the specified direction once before closing upon itself, will do so always at the same point, which is an equilibrium point of the *Poincaré map*. If the periodic orbit happens to pierce $\mathbf{S}_p$ T times before closing upon itself, it will do so at period-T points of the *Poincaré map*. Thus, the problem of detecting a periodic orbit of an n-dimensional continuous-time system is converted to finding a periodic point of an $(n-1)$-dimensional discrete-time system. In Figure 2.2, a 2D Poincaré surface of section and piercing points for a 3D system are shown.

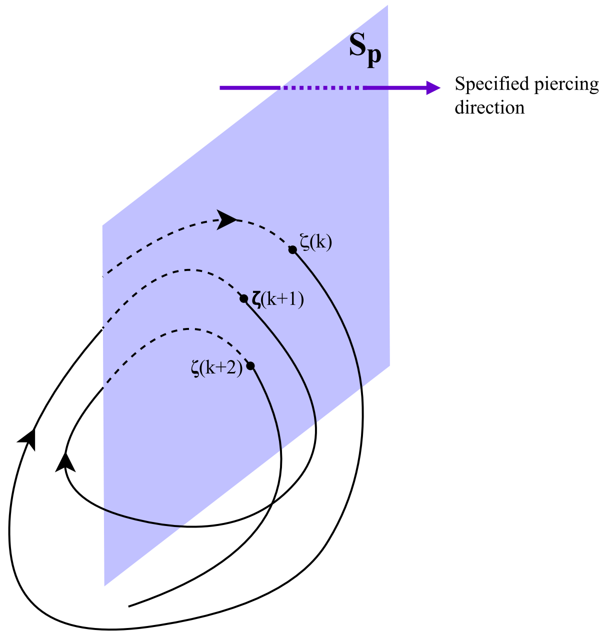

Figure 2.2. Poincaré surface of section for 3D space

Considering an autonomous system of the form Equation 2.1, let $E(\mathbf{w})$ be a real-valued continuous function that is non-constant on every open set, and remains constant along system trajectories. This implies that

$$\dot{E}(\mathbf{w}) = \nabla E(\mathbf{w})\dot{\mathbf{w}} = \nabla E(\mathbf{w})\mathbf{f}(\mathbf{w}) \tag{2.12}$$

If such function $E(\mathbf{w})$, namely a conserved quantity exists for a given system $\dot{\mathbf{w}} = \mathbf{f}(\mathbf{w})$, it is said to be *conservative*. Conversely, if $\dot{E}(\mathbf{w}) \leq 0$ the system is said to be *dissipative*. In a *dissipative system*, trajectories starting from a set of initial conditions which occupies a finite state-space (hyper)-volume converge to an attractor as the state-space (hyper)-volume they occupy shrinks down to zero.

If in a given system nearby trajectories diverge from each other, this implies that the system will exhibit sensitive dependence on initial conditions and long term unpredictability. To be more specific, if there exists a small uncertainty regarding the location of the initial point of a trajectory, the actual trajectory and estimated trajectory lead to growing prediction error. Of particular interest are dissipative systems that exhibit such a property. This may seem paradoxical, because dissipativity implies convergence of nearby trajectories, while sensitive dependence on initial conditions implies their divergence. However, for continuous dynamical systems of three or higher dimensions, it is possible to satisfy both properties, because convergence and divergence behavior can be exhibited along different directions. If convergence behavior in some directions dominates the divergence behavior in other directions such that state-space (hyper) volumes shrink as time evolves, the system will still be a dissipative one. Such dissipative systems where nearby trajectories diverge from each other at least in one direction are *dissipative chaotic systems.* The convergence-divergence behavior of nearby trajectories can be expressed in terms of *Lyapunov exponents.* An n dimensional system has n *Lyapunov exponents* corresponding to the exponential rate of divergence or convergence of nearby trajectories in the associated directions. *Chaotic systems* have at least one positive *Lyapunov exponent* indicating divergence in at least one direction. Attractors of dissipative chaotic systems, the so-called strange attractors, have typically fractal structure and are confined to a finite region.

The strange attractor of the Lorenz system [1] for parameters $\sigma = 10$, $\rho = 28$ and $\beta = 8/3$ and the Rössler system [5] for parameters $a = 0.2$, $b = 0.2$ and $c = 9$ are shown in Figure 2.3.

As a typical feature, *strange attractors* harbor infinitely many UPOs. It should be noted that these UPOs have saddle type of instability which means that the UPO attracts trajectories in one direction and repels them in other directions. Thus, the behavior on a strange attractor can be envisaged as an irregular rambling between the UPOs embedded on the *strange attractors.* Most of the studies on chaotic systems are related to the steady state behavior on the strange attractor, because the transient behavior until the system reaches the attractor is only short-lived.

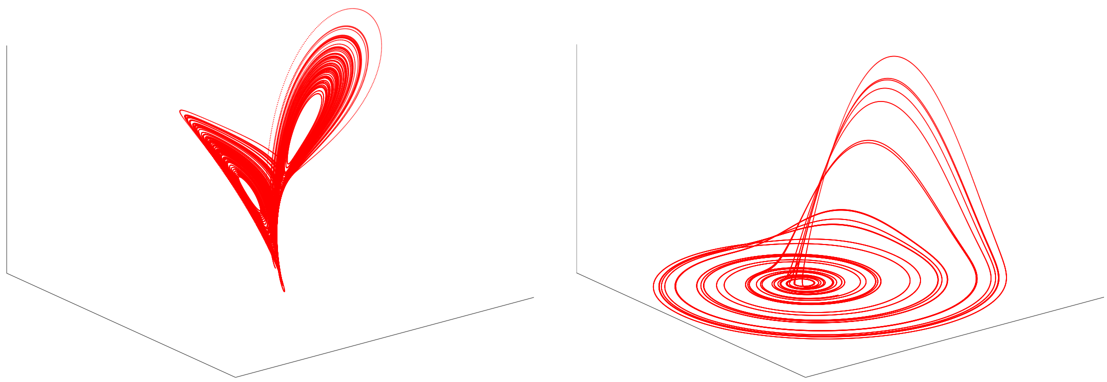

(a) The Lorenz attractor (b) The Rössler attractor

Figure 2.3. Strange attractors

2.2. Synchronization

As mentioned earlier, if two or more oscillators arrange their feature(s) of oscillations due to mutual interaction or under the effect of an outside excitation they are said to be synchronized. Synchronization of coupled systems depends on how they are coupled. The coupling structure has two different features:

(i) the coupling configuration

(ii) how the coupling variable affects the dynamics of the coupled systems

Coupling of two systems may consist of the influence of one upon the other. Such a *unidirectional coupling* is also referred to as *master-slave* coupling or *drive-response* coupling in the literature. Conversely, both systems can mutually influence each other amounting to a *bidirectional coupling*. If there exist several systems, different alternatives are possible depending on the existence and directionality of a link between any pair of systems. Well-known coupling schemes in the literature include *ring coupling*, *star coupling*, *all-to-all coupling*, *nearest neighbor coupling* and *open ring coupling* (Figure 2.4).

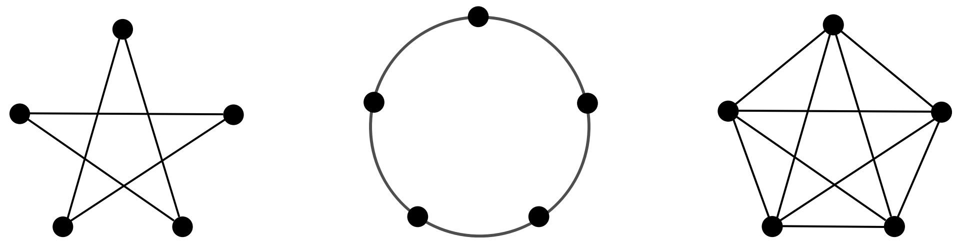

(a) Star (b) Ring (c) All-to-all

Figure 2.4. Sample Coupling Configurations of Networks

In a network of N systems, the coupling scheme can be compactly represented in terms of an $N \times N$ binary coupling matrix:

$$\Gamma = \begin{pmatrix} \gamma_{11} & \gamma_{12} \\ \gamma_{21} & \gamma_{22} \end{pmatrix}$$

the ij^{th} element of which is 1 if i^{th} system affects the j^{th} system, and 0 otherwise. In its most general form the influence of the other systems states on the i^{th} system can be shown as follows

$$\dot{\mathbf{w}}_i = \mathbf{F}_i(\mathbf{f}_i(\mathbf{w}_i), \boldsymbol{\mu}_i(\mathbf{w}_1, \ldots, \mathbf{w}_N)) \qquad i = 1, \ldots, N \tag{2.13}$$

where $\boldsymbol{\mu}_i(\mathbf{w}_1, \ldots, \mathbf{w}_N)$ is the vector of coupling variables influencing the i^{th} system, and $\mathbf{F}_i$ is the function that specifies how the dynamics of the i^{th} system is affected by $\boldsymbol{\mu}_i$.

2.2.1. Some Common μ-Functions for Coupling Two Systems

Although different context may require different coupling variables, here some commonly used $\boldsymbol{\mu}$-functions are presented.

<u>2.2.1.1. Weighted Average of Full-State Vectors.</u> For two coupled systems such a μ-function can be expressed as

$$\boldsymbol{\mu}_i(\mathbf{w}_i, \mathbf{w}_j) = (1-\epsilon_i)\mathbf{w}_i + \epsilon\mathbf{w}_j \qquad i = 1,2 \qquad \mathit{and} \qquad i \neq j \tag{2.14}$$

where $\boldsymbol{\mu}_i$ is an n-dimensional coupling variable and ϵ_i is the *influence coefficient.*

An important special case corresponds to $\epsilon_i = 0.5$, which is the so-called *mean-field coupling of full states*

$$\boldsymbol{\mu}_i(\mathbf{w}_i, \mathbf{w}_j) = \hat{\mathbf{w}}_i = \hat{\mathbf{w}}_j = \frac{\mathbf{w}_i + \mathbf{w}_j}{2} \qquad i = 1,2 \tag{2.15}$$

where $\hat{\mathbf{w}}_i$ is the coupling variable calculated by the function $\boldsymbol{\mu}_i$.

It should be noted that the generalization of this $\boldsymbol{\mu}$-function to multi-system coupling needs to be expressed as follows

$$\boldsymbol{\mu}_i(\mathbf{w}_1, \ldots, \mathbf{w}_N) = \mathbf{W}_i[\mathbf{w}_1, \ldots, \mathbf{w}_N]^\top \quad i = 1, \ldots, N \tag{2.16}$$

where $\mathbf{W}_i$ is the $N{\times}N$ row-stochastic weighting matrix of the i^{th} system. If this notation is applied to a 2-system combination, the i^{th} diagonal entry of $\mathbf{W}_i$ is equal to ϵ_i.

<u>2.2.1.2. Weighted Average of a Subset of States.</u> Here, only a sunset of state variables are used for calculating the vector of coupling variables. For two coupled systems such a $\boldsymbol{\mu}$-function can be expressed as

$$\mu_i(\mathbf{w}_i, \mathbf{w}_j) = \hat{\mathbf{w}}_i = (1-\epsilon_i)\mathbf{S} \quad \mathbf{w}_i + \epsilon_i\mathbf{S} \quad \mathbf{w}_j \qquad i,j = 1,2 \quad \text{and} \quad i \neq j \tag{2.17}$$

where $\hat{\mathbf{w}}_i$ is an m dimensional vector of coupling variables and $\mathbf{S}$ is an $m \times n$ *state selection matrix* $(m < n)$. Choosing $\epsilon_i = 0.5$ corresponds to *mean-field coupling of selected states.*

2.2.1.3. Difference of Full-State Vectors. For two coupled systems $\boldsymbol{\mu}$-function can be expressed as

$$\mu_i(\mathbf{w}_1, \mathbf{w}_2) = \hat{\mathbf{w}}_i = \mathbf{w}_j - \mathbf{w}_i \qquad i = 1, 2 \quad \text{and} \quad i \neq j \tag{2.18}$$

$\boldsymbol{\mu}$-function can be generalized for N coupled systems as

$$\mu_i(\mathbf{w}_1, \ldots, \mathbf{w}_N) = \hat{\mathbf{w}}_i = \sum_{j=1}^{N} W_i(\mathbf{w}_j - \mathbf{w}_i) \qquad i = 1, \ldots, N \quad \text{and} \quad i \neq j \tag{2.19}$$

2.2.1.4. Difference of a Subset of States. It is also possible to work with a $\boldsymbol{\mu}$-function that consists of the difference of some selected state variables of the coupled systems. For two coupled systems the $\boldsymbol{\mu}$-function can be expressed as

$$\boldsymbol{\mu}_i(\mathbf{w}_1, \mathbf{w}_2) = \hat{\mathbf{w}}_i = \mathbf{S}(\mathbf{w}_j - \mathbf{w}_i) \qquad i = 1, 2 \quad \text{and} \quad i \neq j \tag{2.20}$$

2.2.2. Some Common F-Functions for Coupling Two Systems

As can be seen from Equation 2.13, the F- function represents the effect of the coupling variables on coupled system dynamics. Here, commonly used F- functions are presented.

2.2.2.1. Replacement of a Subset of States. The vector of coupling variables calculated by the $\boldsymbol{\mu}$-function can replaced a subset of the states. In this case, the coupled system dynamics can be expressed as

$$\begin{aligned} \dot{\mathbf{w}}_i &= \mathbf{F}_i(\mathbf{f}_i(\mathbf{w}_i), \boldsymbol{\mu}_i(\mathbf{w}_1, \ldots, \mathbf{w}_N)) \\ &= \mathbf{F}_i(\mathbf{f}_i(\hat{\mathbf{w}}_i)) \qquad i = 1, \ldots, N \end{aligned} \tag{2.21}$$

where

$$\hat{\mathbf{w}}_i = (\mathbf{I} - \mathbf{S}^\top\mathbf{S})[\mathbf{w}_1, \ldots, \mathbf{w}_N]^\top + \mathbf{S}^\top\boldsymbol{\mu} \tag{2.22}$$

and $\mathbf{S}$ is an $m \times n$ state selection matrix.

<u>2.2.2.2. Additive Linear Coupling.</u> The vector of coupling variables calculated by the $\boldsymbol{\mu}$-function can be added to the system dynamics as follows

$$\begin{aligned} \dot{\mathbf{w}}_i &= \mathbf{F}_i(\mathbf{f}_i(\mathbf{w}_i), \boldsymbol{\mu}_i(\mathbf{w}_1, \ldots, \mathbf{w}_N)) \\ &= \mathbf{f}_i(\mathbf{w}_i) + \nu\mathbf{S}^\top\boldsymbol{\mu} \qquad\qquad i = 1, \ldots, N \end{aligned} \tag{2.23}$$

where $\mathbf{S}$ is an $m \times n$ state selection matrix.

2.3. Synchronization of Two Oscillators

Synchronous behavior depends on which feature(s) of the coupled systems are in harmony. When two oscillators are suitably coupled, different types of synchronization can occur. Particular type of synchronization that is used in thesis is *complete synchronization* (CS) (or *identical synchronization*) which denotes the perfect synchronization of all state variables and phases of the oscillators in the network [36, 48]. For two coupled systems, *CS* is achieved if Equation 2.24 is satisfied.

$$\lim_{t\to\infty} \|\mathbf{w}_1(t) - \mathbf{w}_2(t)\| = \mathbf{0} \tag{2.24}$$

$\mathbf{w}_1(t) = \mathbf{w}_2(t)$ is the *synchronization manifold* where the synchronous behavior converges in the long run. Stability on the *synchronization manifold* determines the ability to synchronize. Several other types of synchronization are presented in Appendix C.

2.4. Decomposition Based Synchronization of Coupled Chaotic Systems

As mentioned earlier, Pecora and Carroll were the first to show that under certain conditions it is possible to achieve complete synchronization as in Equation 2.24 for coupled identical chaotic oscillators in the form of 2.25 [36]. Various coupling configurations and conditions are proposed in the literature since the 1990 paper [36] by Pecora and Carroll. Cuomo and Oppenheim applied the work of Pecora and Carroll to electronic circuits in 1993 [37]. As mentioned previously, the investigated synchronization in this thesis is CS as specified in Equation 2.24. The decomposition based synchronization method proposed by Pecora and Carroll [36, 37, 49, 50] briefly is explained below.

In order to guarantee the synchronizability of two identical n-dimensional chaotic systems,

$$\dot{\mathbf{w}}_1 = \mathbf{f}(\mathbf{w}_1) \quad \text{and} \quad \dot{\mathbf{w}}_2 = \mathbf{f}(\mathbf{w}_2) \qquad \mathbf{w}_1, \mathbf{w}_2 \in R^n \tag{2.25}$$

$\mathbf{f}(\mathbf{w})$ has to be decomposable into a k-dimensional *drive subsystem* and a l-dimensional stable *response subsystem*,

$$\text{drive subsystem :} \qquad \dot{\mathbf{q}} = \mathbf{g}(\mathbf{q}, \mathbf{v}) \qquad \mathbf{q} \in R^k \tag{2.26}$$

$$\text{stable response subsystem :} \qquad \dot{\mathbf{v}} = \mathbf{h}(\mathbf{q}, \mathbf{v}) \qquad \mathbf{v} \in R^l \tag{2.27}$$

where $\mathbf{w} = [\mathbf{q}, \mathbf{v}]^\top$ and $\mathbf{f} = [\mathbf{g}, \mathbf{h}]^\top$.

Assume now that the two identical systems are coupled in such a way that the first system is the master ($\mathbf{w}_m = \mathbf{w}_1$) and the second one is the slave ($\mathbf{w}_s = \mathbf{w}_2$). The vector of coupling variables, $\boldsymbol{\mu}$, is taken as the selected state $\mathbf{q}_m$:

$$\boldsymbol{\mu}(\mathbf{w}_m) = \hat{\mathbf{q}} = \mathbf{q}_m \tag{2.28}$$

which is fed into the response subsystem of the slave to provide complete replacement of $\mathbf{q}_s = \boldsymbol{\mu} = \hat{\mathbf{q}} = \mathbf{q}_m$.

Provided that the response system is stable, this coupling configuration (Figure 2.5) guarantees robust synchronization of the slave to the master.

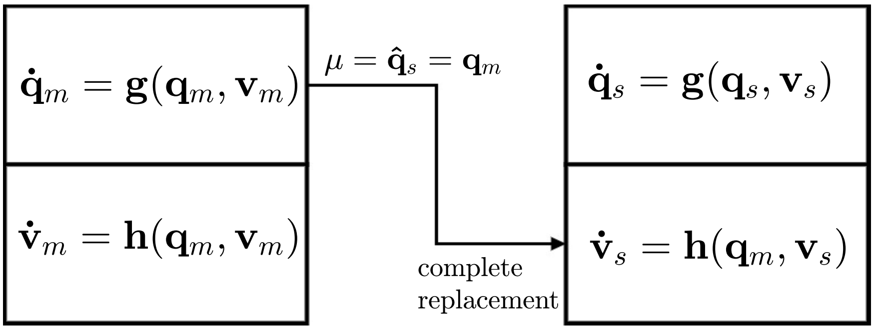

Figure 2.5. Decomposition-based master-slave coupling

With such a coupling, the combination of two n dimensional systems becomes a single $2n - m$ dimensional system. This method can be applied to two coupled Lorenz systems [1] as given in Equation 3.8. In [36, 49], it is shown that the Lorenz system can be decomposed into a drive and a stable response system in two different ways, where wither x component or the z component can be used as the drive. In Equation 2.29, the master-slave coupling is given with the x component as the drive. Resulting synchronization behavior is presented in Figure 2.6 where the coupling is activated at $t = 20\,sec$. As it can be seen, synchronization is achieved rapidly and is robust.

$$\begin{pmatrix} \dot{x}_1 = 10(y_1 - x_1) \\ \dot{y}_1 = 28x_1 - y_1 - x_1 z_1 \\ \dot{z}_1 = x_1 y_1 - 8/3 z_1 \end{pmatrix} \quad \text{and} \quad \begin{pmatrix} \dot{x}_2 = 10(y_2 - x_2) \\ \dot{y}_2 = 28x_1 - y_2 - x_1 z_2 \\ \dot{z}_2 = x_1 y_2 - 8/3 z_2 \end{pmatrix} \tag{2.29}$$

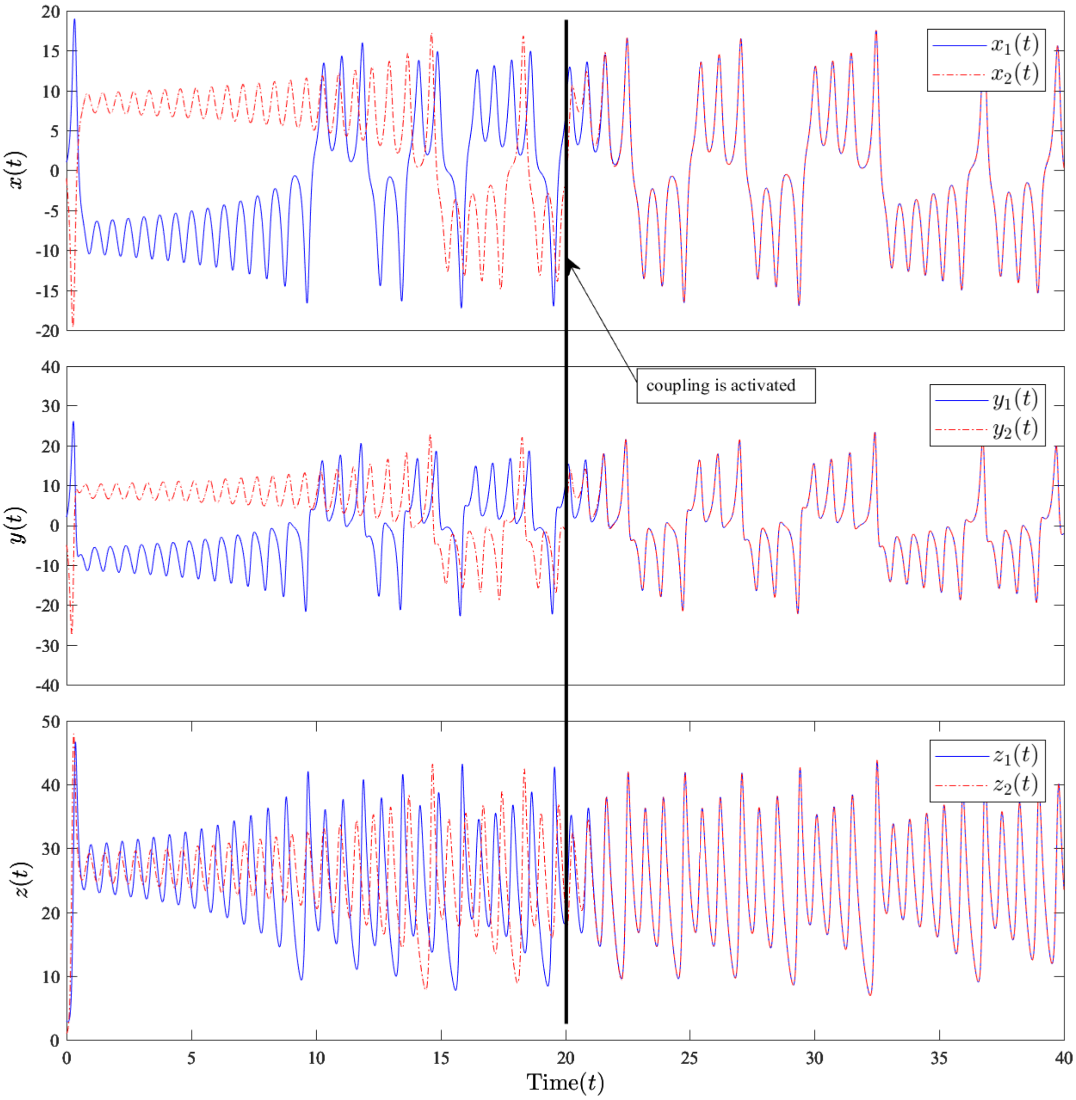

Figure 2.6. Synchronization of two Lorenz systems which are master-slave coupled using the x-state as the drive component

2.5. Chaos Control via OGY Method

Controlling chaos via small parameter perturbations has first been suggested by Ott Grebogi and Yorke in 1990. The key idea of OGY control is to select one of the infinitely many UPOs embedded in the strange attractor as the target and stabilizing it through small parameter changes. OGY control is applied at discrete time instants when the system trajectories transverses a chosen Poincaré surface in the specified direction. Thus, the control input consists of the shift of one or more system parameters from their nominal values.

The OGY method is applicable to the systems of the form Equation 2.1 or Equation 2.2 which have at least one adjustable parameter that can be slightly varied for control purposes. For a continuous-time chaotic system of the form Equation 2.1, first, a suitable Poincaré surface, S_p, has to be chosen and the associated Poincaré map, $\mathbf{P}$, (Equation 2.11) has to be obtained empirically. Next, one of the UPOs transversing S_p has to be chosen as the target UPO to be stabilized. Such UPOs pierce S_p at $\boldsymbol{\zeta}$-points which correspond to periodic points of the associated Poincaré map

$$\boldsymbol{\zeta}(k) = \boldsymbol{\zeta}(k+T) = \boldsymbol{\zeta}_i^{*T} \qquad i = 1, \ldots, T \tag{2.30}$$

where $\boldsymbol{\zeta}$ is the state vector, $\{\boldsymbol{\zeta}_i^{*T}; i = 1, \ldots, T$ are the points where a UPO pierces S_p and T is the number of times the chosen UPO pierces S_p in the specified direction before closing upon itself.

In their (1990) original paper, Ott, Grebogi and Yorke proposed control via a single parameter, however, OGY method has later been extended to multi-parameter case [17]. In this case, the control input $\mathbf{u}$ consist of the deviations of m system parameters from their nominal values.

$$\mathbf{u} = \mathbf{p} - \mathbf{p}_{nom} \tag{2.31}$$

These derivations are not allowed to exceed a predefined small threshold value.

$$|\mathbf{u}_i| = |\mathbf{p}_i - \mathbf{p}_{i,nom}| \leq \delta_i \qquad i = 1, \ldots, m \tag{2.32}$$

Thus, the control parameter vector $\mathbf{p}$ is confined to the parameter space region $\Pi = \{\mathbf{p} \in R^m : p_{i,nom} - \delta_i \leq p_i \leq p_{i,nom} + \delta_i, \forall i = 1, \ldots, m\}$, which guarantees that the modification of the control parameters does not alter the chaotic nature of the nominal system.

Although also applicable for the stabilization of UPOs, which pierce S_p multiple times before closing upon themselves, for the sake of simplicity, let us introduce OGY method for a UPO, which pierces in the specified direction only at a single point $\boldsymbol{\zeta}^*$.

The control law devised by the OGY method is based on a local linear approximation of the Poincaré map in a close neighborhood of $\boldsymbol{\zeta}^*$ called the OGY region (Ω_{OGY}).

$$\boldsymbol{\zeta}(k+1) = \mathbf{P}(\boldsymbol{\zeta}(k), \mathbf{p}(k)) \cong \mathbf{A}\boldsymbol{\zeta}(k) + \mathbf{B}\mathbf{p}(k) \quad \text{for} \quad \boldsymbol{\zeta} \in \Omega_{OGY}, \quad \mathbf{p} \in \Pi \tag{2.33}$$

where $\boldsymbol{\zeta}(k)$ is the point where the system trajectories pierces the Poincaré surface for the k^{th} time, and $\mathbf{p}(k)$ is the vector of control parameters, as it will be set from the k^{th} piercing until the $(k+1)^{th}$ piercing. The OGY region is typically taken in spherical (or circular in case of a 2-dimensional Poincaré surface) form and is specified in terms of its radius ($\Omega_{OGY} = \{\forall\boldsymbol{\zeta} : \|\boldsymbol{\zeta} - \boldsymbol{\zeta}^*\| \leq R_{OGY}\}$). $\mathbf{A}$ and $\mathbf{B}$ matrices are related to the Poincaré map as follows:

$$\begin{aligned} \mathbf{A} &= \frac{\partial \mathbf{P}(\boldsymbol{\zeta}, \mathbf{p})}{\partial \boldsymbol{\zeta}}|_{\boldsymbol{\zeta}=\boldsymbol{\zeta}^*, \mathbf{p}=\mathbf{p}_{nom}} \\ \mathbf{B} &= \frac{\partial \mathbf{P}(\boldsymbol{\zeta}, \mathbf{p})}{\partial \mathbf{p}}|_{\boldsymbol{\zeta}=\boldsymbol{\zeta}^*, \mathbf{p}=\mathbf{p}_{nom}} \end{aligned} \tag{2.34}$$

Nevertheless, instead of first obtaining the Poincaré map empirically and then calculating the $\mathbf{A}$ and $\mathbf{B}$ matrices according to Equation 2.34, it is more practical to estimate $\mathbf{A}$ and $\mathbf{B}$, which make empirical data fit into the linear model in 2.33.

If the linearized system in Equation 2.33 is controllable, any standard linear method can be used to design the *control matrix*, $\mathbf{K}$, to be used in the linear control law, $\mathbf{u}_{lin}$

$$\mathbf{u}_l in = -\mathbf{K}(\boldsymbol{\zeta}(k) - \boldsymbol{\zeta^*}) \tag{2.35}$$

such that the deviation $\boldsymbol{\eta} = \boldsymbol{\zeta}(k) - \boldsymbol{\zeta^*}$ is stabilized at $\mathbf{0}$. This requires that in the closed-loop deviation dynamics governed by where $\mathbf{K}$ is the control matrix and $\boldsymbol{\zeta^*}$ is the piercing point of the UPO. Using $\boldsymbol{\eta} = \boldsymbol{\zeta}(k) - \boldsymbol{\zeta^*}$, controlled system will be expressed as

$$\begin{aligned} \boldsymbol{\eta}(k+1) &= \mathbf{A}\boldsymbol{\eta}(k) - \mathbf{BK}\boldsymbol{\eta}(k) \\ &= (\mathbf{A} - \mathbf{BK})\boldsymbol{\eta}(k) \end{aligned} \tag{2.36}$$

the eigenvalues of $(\mathbf{A} - \mathbf{BK})$ remain within the unit circle. It should be noted that the chosen $\mathbf{K}$ must also guarantee that $\mathbf{u}_l in$ obtained by Equation 2.35 satisfies the bounds on parameter variation given in Equation 2.36 $\forall \boldsymbol{\zeta} \in \Omega_{OGY}$. As a matter of fact, this can be achieved easily by sufficiently reducing the radius of Ω_{OGY}.

So, with the appropriate design of $\mathbf{K}$, the OGY control law,

$$\mathbf{u}_{OGY} = \begin{cases} -\mathbf{K}(\boldsymbol{\zeta} - \boldsymbol{\zeta}^*) & \text{if } \boldsymbol{\zeta} \in \Omega_{OGY}; \\ \mathbf{0} & \text{if } \boldsymbol{\zeta} \notin \Omega_{OGY}; \end{cases} \tag{2.37}$$

specifies how the control parameter vector $\mathbf{p} = \mathbf{p}_{nom} + \mathbf{u}_{OGY}$ will be altered depending on $\boldsymbol{\zeta}$, the most recent point where the system trajectory has pierced the Poincaré surface in the specified direction.

According to Equation 2.37, the system trajectory will ramble on the strange attractor until it pierces S_p at a point $\boldsymbol{\zeta} \in \Omega_{OGY}$, which is bound the happen within finite time due to the *ergodic* nature of the chaotic motion on the strange attractor. From that time instance onward, the control activity will keep the trajectory *trapped* on the target UPO.

So far, OGY control has been described for a target UPO, which closes upon itself after piercing S_p once in the specified direction. For the stabilization of a target UPO, which closes after T piercings, the method can be easily generalized; namely instead of a period-1 point, a period-T point of the Poincaré map will be stabilized in a similar manner and parameter vector $\mathbf{p}$ will be updated at every T^{th} piercing. For details of the OGY method the reader is recommended to refer to [51].

Since the continuous-time system is numerically simulated, the detection of the exact points where the continuous trajectory pierces the Poincaré surface is difficult. To overcome this difficulty, different numerical approaches can be used, some of which are given in Appendix C.

The basic OGY method is demonstrated below for two examples, (i) the Logistic map and (ii) the Henon map.

(i) The Logistic equation which was published by May in 1976 is a 1D nonlinear map representing the discrete time population dynamics [3]. The Logistic map is defined by Equation 2.38.

$$x(k+1) = a\,x(k)[1 - x(k)] \quad x(k) \in [0, 1] \tag{2.38}$$

where x is the state of the system and a is the parameter. It exhibits chaotic behavior for certain values of the parameter a and has two two equilibrium points which are defined as

$$
\begin{aligned}
{x_1}^* &= 0 \\
{x_2}^* &= \frac{a-1}{a}
\end{aligned}
\tag{2.39}
$$

The Logistic map with $a_{nom} = 3.9$ is stabilized by basic OGY method at $x^* = 0.745$ using a as the control parameter. Figure 2.7 shows the system states and the control parameter variations when OGY control is applied within a small OGY region with $R_{OGY} = 0.001$ and with parameter perturbations $|\Delta a| \leq 0.001$. Figure 2.8 shows the same variables for a larger OGY region $R_{OGY} = 0.01$ and larger parameter perturbations $|\Delta a| \leq 0.1$. As can be seen from the figures, increasing the size of the OGY region and the range of the control parameter results in a faster activation of the OGY control and stabilization of the target. However, these parameters cannot be increased arbitrarily. The size of the OGY region has to be limited in order to keep local linearization valid. Similarly, the control parameter variations have to be confined to a range within which the system dynamics does not change its chaotic character..

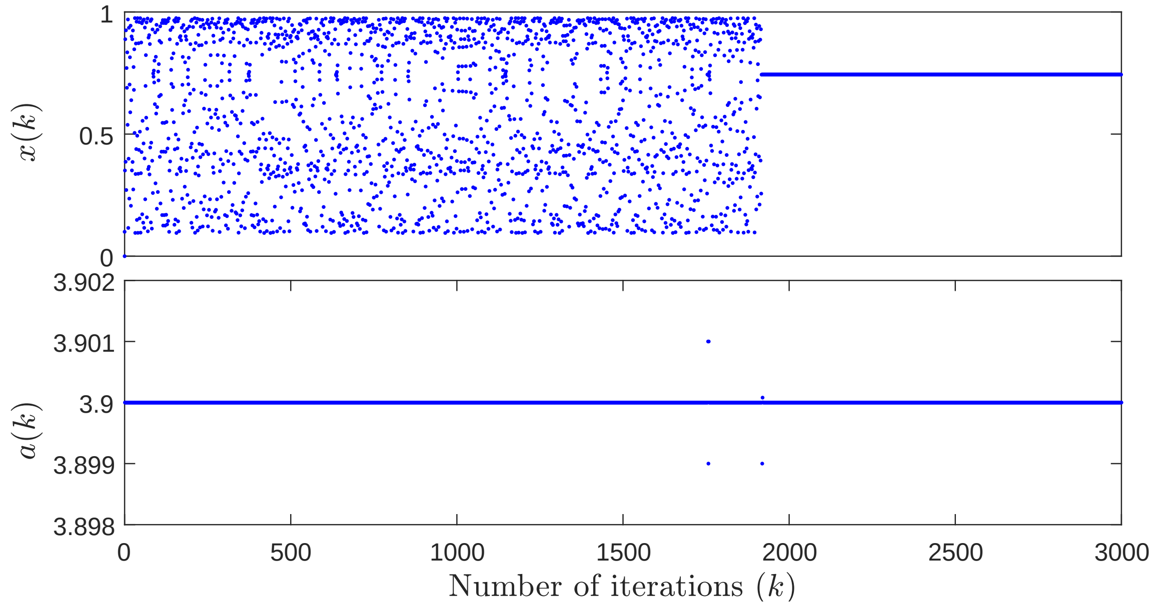

Figure 2.7. OGY control of the Logistic map with $a_{nom} = 3.9$, and the target $x^* = 0.745$, $\Delta a = 0.001$ and $R_{OGY} = 0.001$

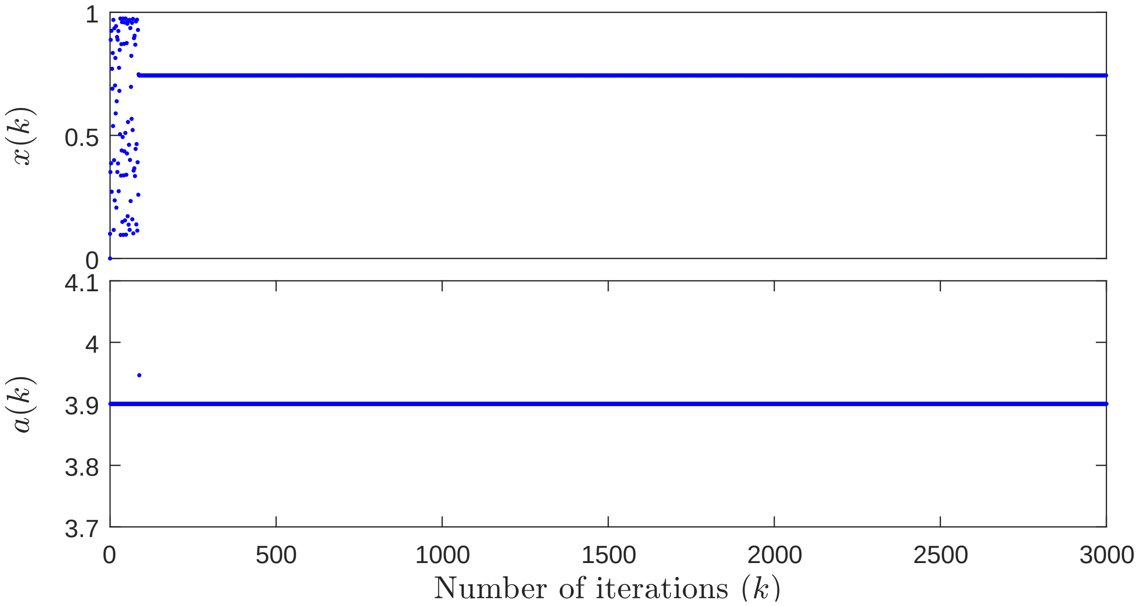

Figure 2.8. OGY control of the Logistic map with $a_{nom} = 3.9$, and the target $x^* = 0.745$, $\Delta a = 0.1$ and $R_{OGY} = 0.01$

(ii) The Henon map is a 2D nonlinear discrete mathematical model published by Henon in 1976 [4]. The Henon map also exhibits chaotic behavior for some range of the parameter values.

$$\begin{aligned} x(k+1) &= a + b\,y(k) - x(k)^2 \\ y(k+1) &= x(k) \end{aligned} \tag{2.40}$$

where $\mathbf{w}(k) = [x(k),\, y(k)]^\top$ is the state vector and a and b are the system parameters. The Henon map has two equilibrium points which are defined as

$$({x_{1,2}}^*, {y_{1,2}}^*) = \left(\frac{(b-1) \mp \sqrt{(b-1)^2 + 4a}}{2}, \frac{(b-1) \mp \sqrt{(b-1)^2 + 4a}}{2} \right) \tag{2.41}$$

The Henon map with $(a_{nom}, b_{nom}) = (1.37, 0.3)$ is stabilized by the basic OGY method at $\mathbf{w}^* = [0.8717, 0.8717]^\top$ using a as the control parameter with $|\Delta a| \leq 0.03$. Figure 2.9 shows the system states and the control parameter variation when OGY control is applied within a small OGY region with $R_{OGY} = 0.2$.

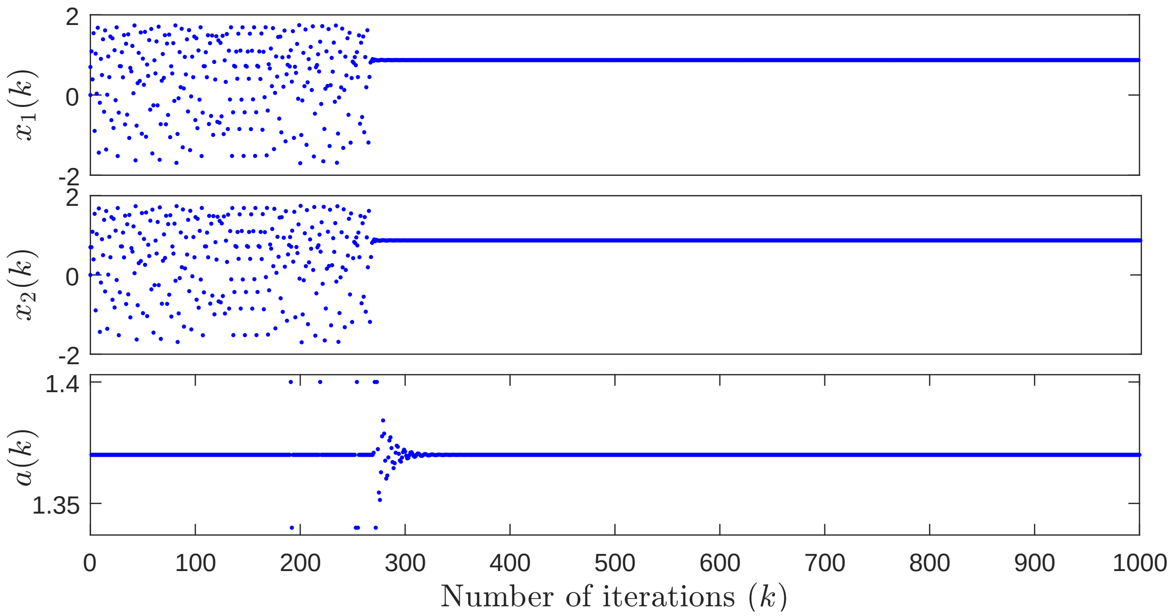

Figure 2.9. OGY Control of the Henon map with $(a_{nom}, b_{nom}) = (1.37, 0.3)$, and target $\mathbf{w}^* = [0.877, 0.877]^\top$, $\Delta a = 0.03$ and $R_{OGY} = 0.2$

Since Ott, Grebogi and Yorke published their article in 1990, various extensions and modifications of their method are proposed. Nitsche and Dressler in 1992 [12] extended the basic OGY method using delay coordinates for the system which have unknown dynamic and this approach is applied to the experimental systems successfully [8]. A multiparameter case extension of OGY method, which allows faster stabilization and robustness against the noise, is suggested by Barretto and Grebogi in 1995 [17]. In 1992, Romeras et al extended the method for higher dimensional systems with a general feedback form [16]. Also, targeting techniques to reduce the time to start the control procedure are proposed in the literature [52–55]. Since, CS-OGY, which is a slightly modified version of the basic OGY method, only general information about the extensions are provided here. In [51, 56, 57] details of the above mentioned and additional extensions of OGY method are presented.

3. INVESTIGATION OF DIFFERENT COUPLING CONFIGURATIONS FOR DECOMPOSITION BASED CHAOS SYNCHRONIZATION

In Chapter 2, the decomposition based chaos synchronization method as proposed by Pecora and Carroll has been explained in detail. As can be seen, Pecora and Carroll have used a master-slave type coupling configuration with complete replacement of the *drive* states in the *response* system of the *slave*. However, in this thesis, it is intended to allow both unidirectional and bidirectional coupling, and to use coupling variable consisting of a weighted average of selected states.

Consider two identical chaotic systems

$$\dot{\mathbf{w}}_1 = \mathbf{f}(\mathbf{w}_1) \quad \text{and} \quad \dot{\mathbf{w}}_2 = \mathbf{f}(\mathbf{w}_2) \qquad \mathbf{w}_1, \mathbf{w}_2 \in \mathbf{R}^n \tag{3.1}$$

which can be decomposed into

$$\begin{pmatrix} \text{drive}_1 : & \dot{\mathbf{q}}_1 = \mathbf{g}(\mathbf{q}_1, \mathbf{v}_1) \\ \text{response}_1 : & \dot{\mathbf{v}}_1 = \mathbf{h}(\mathbf{q}_1, \mathbf{v}_1) \end{pmatrix} \quad \text{and} \quad \begin{pmatrix} \text{drive}_2 : & \dot{\mathbf{q}}_2 = \mathbf{g}(\mathbf{q}_2, \mathbf{v}_2) \\ \text{response}_2 : & \dot{\mathbf{v}}_2 = \mathbf{h}(\mathbf{q}_1, \mathbf{v}_2) \end{pmatrix} \tag{3.2}$$

where $\mathbf{w} = [\mathbf{q}, \mathbf{v}]^\top$, $\mathbf{f} = [\mathbf{g}, \mathbf{h}]^\top$ and the response subsystems are stable.

Here, the weighted average of the drive components of the coupled systems will be considered as the coupling vector $\boldsymbol{\mu}_i$ acting on the i^{th} system,

$$\boldsymbol{\mu}_i = \hat{\mathbf{q}}_i = (1-\epsilon)\mathbf{q}_i + \epsilon\mathbf{q}_j \qquad i, j = 1, 2 \quad \& \quad i \neq j \tag{3.3}$$

where ϵ is the weighting factor.

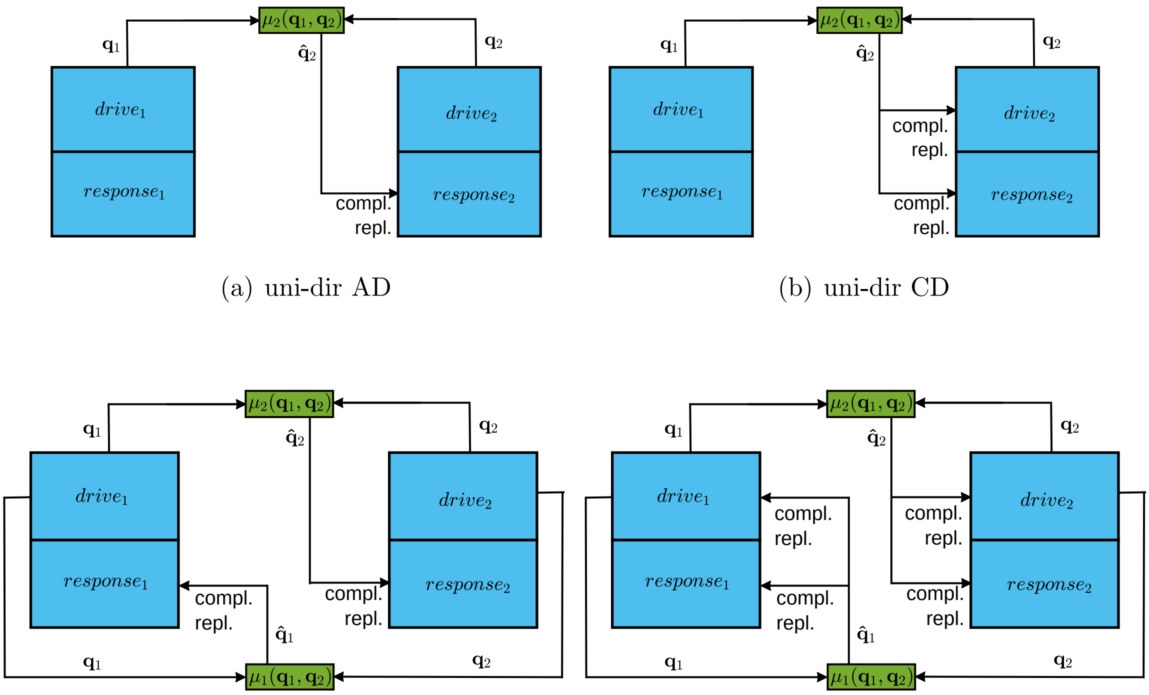

(a) uni-dir AD

(b) uni-dir CD

(c) bi-dir AD

(d) bi-dir CD

Figure 3.1. Four possible coupling configurations

In the original method of Pecora and Carroll the coupling variable affects only the response subsystem of the slave system, while the drive subsystem of the slave remains autonomous. In this thesis this configuration will be referred to as the *autonomous drive* (AD) configuration. On the other hand, it is also possible to feed the coupling variable into both the response and the drive subsystems of the slave, which will be called the *coupled drive* (CD) configuration.

3.1. Considered Coupling Configurations

Alternatives of unidirectional and bidirectional coupling together with the alternatives of AD and CD coupling provide four possible configurations, shown in Figure 3.1.

(i) Unidirectional Coupling with Autonomous Drive (uni-dir-AD)

$$\dot{\mathbf{w}}_1 = \begin{bmatrix} \dot{\mathbf{q}}_1 \\ \dot{\mathbf{v}}_1 \end{bmatrix} = \begin{bmatrix} \mathbf{g}(\mathbf{q}_1, \mathbf{v}_1) \\ \mathbf{h}(\mathbf{q}_1, \mathbf{v}_1) \end{bmatrix} \quad \text{and} \quad \dot{\mathbf{w}}_2 = \begin{bmatrix} \dot{\mathbf{q}}_2 \\ \dot{\mathbf{v}}_2 \end{bmatrix} = \begin{bmatrix} \mathbf{g}(\mathbf{q}_2, \mathbf{v}_2) \\ \mathbf{h}(\hat{\mathbf{q}}_2, \mathbf{v}_2) \end{bmatrix} \tag{3.4}$$

For $\hat{\mathbf{q}}_2 = \boldsymbol{\mu}_2 = (1-\epsilon)\mathbf{q}_2 + \epsilon\mathbf{q}_1$ with $\epsilon = 1$, this configuration corresponds to what Pecora and Carroll have used in their original paper.

(ii) Bidirectional Coupling with Autonomous Drive (bi-dir-AD)

$$\dot{\mathbf{w}}_1 = \begin{bmatrix} \dot{\mathbf{q}}_1 \\ \dot{\mathbf{v}}_1 \end{bmatrix} = \begin{bmatrix} \mathbf{g}(\mathbf{q}_1, \mathbf{v}_1) \\ \mathbf{h}(\hat{\mathbf{q}}_1, \mathbf{v}_1) \end{bmatrix} \quad \text{and} \quad \dot{\mathbf{w}}_2 = \begin{bmatrix} \dot{\mathbf{q}}_2 \\ \dot{\mathbf{v}}_2 \end{bmatrix} = \begin{bmatrix} \mathbf{g}(\mathbf{q}_2, \mathbf{v}_2) \\ \mathbf{h}(\hat{\mathbf{q}}_2, \mathbf{v}_2) \end{bmatrix} \tag{3.5}$$

(iii) Unidirectional Coupling with Coupled Drive (uni-dir-CD)

$$\dot{\mathbf{w}}_1 = \begin{bmatrix} \dot{\mathbf{q}}_1 \\ \dot{\mathbf{v}}_1 \end{bmatrix} = \begin{bmatrix} \mathbf{g}(\mathbf{q}_1, \mathbf{v}_1) \\ \mathbf{h}(\mathbf{q}_1, \mathbf{v}_1) \end{bmatrix} \quad \text{and} \quad \dot{\mathbf{w}}_2 = \begin{bmatrix} \dot{\mathbf{q}}_2 \\ \dot{\mathbf{v}}_2 \end{bmatrix} = \begin{bmatrix} \mathbf{g}(\hat{\mathbf{q}}_2, \mathbf{v}_2) \\ \mathbf{h}(\hat{\mathbf{q}}_2, \mathbf{v}_2) \end{bmatrix} \tag{3.6}$$

(iv) Bidirectional Coupling with Coupled Drive (uni-dir-CD)

$$\dot{\mathbf{w}}_1 = \begin{bmatrix} \dot{\mathbf{q}}_1 \\ \dot{\mathbf{v}}_1 \end{bmatrix} = \begin{bmatrix} \mathbf{g}(\hat{\mathbf{q}}_1, \mathbf{v}_1) \\ \mathbf{h}(\hat{\mathbf{q}}_1, \mathbf{v}_1) \end{bmatrix} \quad \text{and} \quad \dot{\mathbf{w}}_2 = \begin{bmatrix} \dot{\mathbf{q}}_2 \\ \dot{\mathbf{v}}_2 \end{bmatrix} = \begin{bmatrix} \mathbf{g}(\hat{\mathbf{q}}_2, \mathbf{v}_2) \\ \mathbf{h}(\hat{\mathbf{q}}_2, \mathbf{v}_2) \end{bmatrix} \tag{3.7}$$

The four coupling configurations have been applied to two identical Lorenz systems which are defined by the following set of equations

$$\begin{aligned} \dot{x} &= \sigma(y - x) \\ \dot{y} &= \rho x - y - xz \\ \dot{z} &= xy - \beta z \end{aligned} \tag{3.8}$$

where $\mathbf{w} = [x, y, z]^\top$ is the state vector of the system and σ, ρ and β are system parameters. Here, the most common parameter values $\sigma = 10$, $\rho = 28$ and $\beta = 8/3$ are used, which provide chaotic behavior.

Synchronization is possible in all the configurations given in Eqs. (3.4)-(3.7) depending on the weighting factor ϵ used in the calculation of $\boldsymbol{\mu}$. It is known that both x or y components of the Lorenz system lend themselves for the usage as the drive subsystem in the decomposition based synchronization method. Here, the drive subsystem is chosen as x dynamics such that the following decomposition is obtained

$$\begin{aligned} \text{drive}: &\quad q = x \\ \text{response}: &\quad \mathbf{v} = [y, z]^\top \end{aligned} \tag{3.9}$$

For bi-dir-AD coupling with $\epsilon = 0.5$, the stable synchronization of the coupled Lorenz systems has been proven in Appendix D. For other configurations and different ϵ values, simulations are conducted, the results of which are given in Figures 3.2 - 3.5.

In Table 3.1, the value ranges obtained from the numerical simulations for the coupling coefficient ϵ that allows the investigated coupling configurations to achieve CS are listed.

Table 3.1. Synchronization ranges for investigated coupling configurations

	Synchronization Range
uni-dir-AD	$0.42 < \epsilon < 1$
uni-dir-CD	$0.93 < \epsilon < 1$
bi-dir-AD	$0.31 < \epsilon < 1$
bi-dir-CD	$0.4 < \epsilon < 0.5$

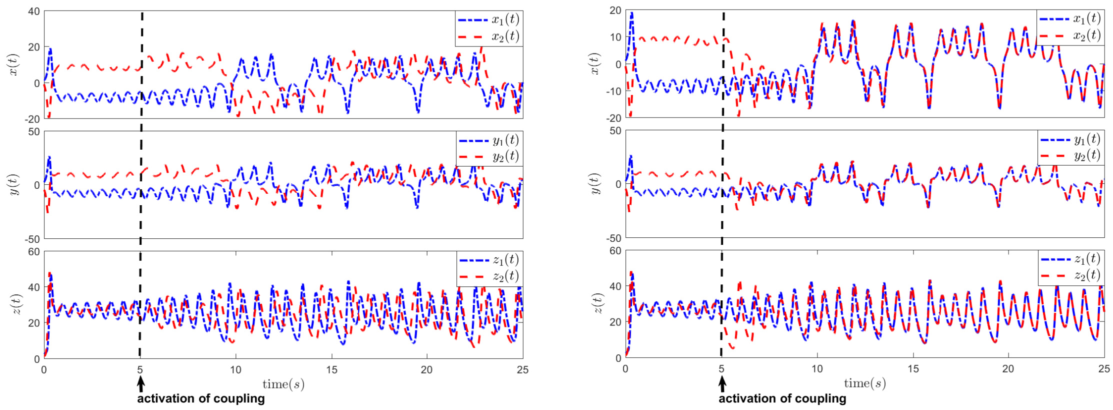

(a) $\epsilon = 0.3$ (Synchronization is not achieved) (b) $\epsilon = 0.5$ (Synchronization is achieved)

Figure 3.2. States of two uni-dir-AD coupled systems (D_1 master, D_2 slave).

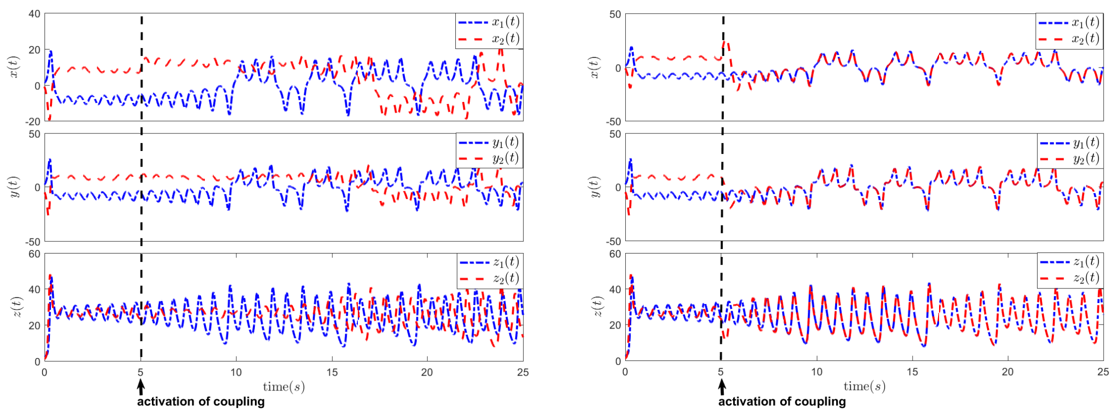

(a) $\epsilon = 0.2$ (Synchronization is not achieved) (b) $\epsilon = 0.9$ (Synchronization is achieved)

Figure 3.3. States of two uni-dir-CD coupled systems (D_1 master, D_2 slave).

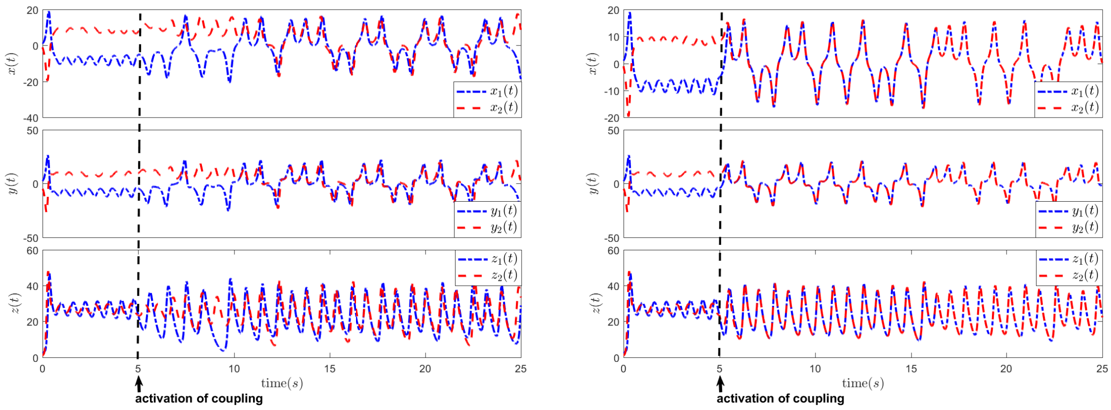

(a) $\epsilon = 0.2$ (Synchronization is not achieved) (b) $\epsilon = 0.5$ (Synchronization is achieved)

Figure 3.4. States of two bi-dir-AD coupled systems.

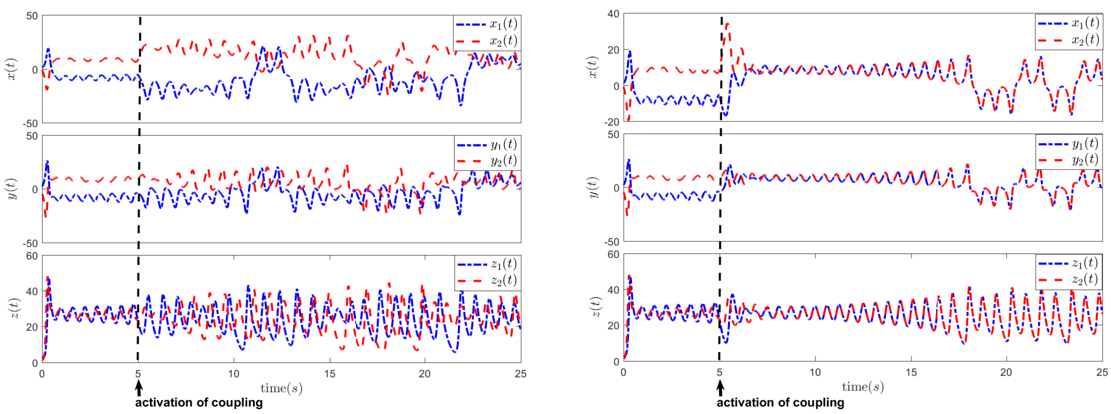

(a) $\epsilon = 0.3$ (Synchronization is not achieved) (b) $\epsilon = 0.45$ (Synchronization is achieved)

Figure 3.5. States of two bi-dir-CD coupled systems.

3.2. Selected Coupling Configuration

The empirical and analytical results summarized in Table 3.1 suggest the most suitable for the purposes of this thesis to be bidirectional coupling with autonomous drive and the usage of mean-field coupling (weighted average with $\epsilon = 0.5$) with full replacement of the drive variable:

$$\dot{\mathbf{w}}_1 = \begin{bmatrix} \dot{\mathbf{q}}_1 \\ \dot{\mathbf{v}}_1 \end{bmatrix} = \begin{bmatrix} \mathbf{g}(\mathbf{q}_1, \mathbf{v}_1) \\ \mathbf{h}(\boldsymbol{\mu}, \mathbf{v}_1) \end{bmatrix} \quad \text{and} \quad \dot{\mathbf{w}}_2 = \begin{bmatrix} \dot{\mathbf{q}}_2 \\ \dot{\mathbf{v}}_2 \end{bmatrix} = \begin{bmatrix} \mathbf{g}(\mathbf{q}_2, \mathbf{v}_2) \\ \mathbf{h}(\boldsymbol{\mu}, \mathbf{v}_2) \end{bmatrix} \tag{3.10}$$

where

$$\boldsymbol{\mu}(\mathbf{q}_1, \mathbf{q}_2) = \hat{\mathbf{q}} = \frac{\mathbf{q_1} + \mathbf{q_2}}{2} \tag{3.11}$$

Also, unidirectional coupling with autonomous drive and the usage of mean-field coupling (weighted average with $\epsilon = 0.5$) with full replacement of the drive variable configuration is used for unidirectional coupling states:

$$\dot{\mathbf{w}}_1 = \begin{bmatrix} \dot{\mathbf{q}}_1 \\ \dot{\mathbf{v}}_1 \end{bmatrix} = \begin{bmatrix} \mathbf{g}(\mathbf{q}_1, \mathbf{v}_1) \\ \mathbf{h}(\mathbf{q}_1, \mathbf{v}_1) \end{bmatrix} \quad \text{and} \quad \dot{\mathbf{w}}_2 = \begin{bmatrix} \dot{\mathbf{q}}_2 \\ \dot{\mathbf{v}}_2 \end{bmatrix} = \begin{bmatrix} \mathbf{g}(\mathbf{q}_2, \mathbf{v}_2) \\ \mathbf{h}(\boldsymbol{\mu}, \mathbf{v}_2) \end{bmatrix} \tag{3.12}$$

where

$$\begin{aligned} \boldsymbol{\mu}_1(\mathbf{q}_1, \mathbf{q}_2) &= \hat{\mathbf{q}}_1 = \mathbf{q_1} \\ \boldsymbol{\mu}_2(\mathbf{q}_1, \mathbf{q}_2) &= \hat{\mathbf{q}}_2 = \frac{\mathbf{q_1} + \mathbf{q_2}}{2} \end{aligned} \tag{3.13}$$

4. PREPARATIONS FOR COMBINING OGY CONTROL AND DECOMPOSITION BASED SYNCHRONIZATION

In this thesis, an original investigation will be conducted on how a small number of identical chaotic systems, which are stabilized at different UPOs by OGY control, can be coupled in such a way that the two tendencies, i. e. the tendency of each system to follow its own distinct UPO and the tendency of coupled systems to synchronize, compete. However, for this purpose some preliminary work is needed: a modification of the OGY method and the development of a selective coupling strategy.

4.1. Control-Saturated OGY Control (CS-OGY)

The classical OGY method which is based on stabilizing a chaotic system at one of its UPOs, slightly modified in this study in order to render it suitable for interaction with a coupling scheme. For the sake of simplicity, this modification will only be explained for a target UPO which closes upon itself after piercing the Poincaré surface only once in the specified direction.

As can be recalled, the original OGY control law has to obey two restrictions: (i) the confinement of the control activity to $\boldsymbol{\zeta} \in \Omega_{OGY}$, where $\boldsymbol{\zeta}$ is the most recent piercing point, (ii) limitation of the magnitude of each control variable according to Equation 2.33. The former restriction is actively imposed as in Equation 2.37, while the latter is indirectly achieved with the appropriate design of $\mathbf{K}$ and limitation of Ω_{OGY}. In the proposed modification the confinement to Ω_{OGY} is released, while the bounds on the magnitude of the control variables are imposed with explicit saturation in the control law. Thus, the modified control law, dubbed as *control saturated* OGY (CS-OGY), can be expressed for the i^{th} control parameter$[\mathbf{u}_{CS-OGY}(\boldsymbol{\zeta})]_i$ as follows:

$$[\mathbf{u}_{CS-OGY}(\boldsymbol{\zeta})]_i = \begin{cases} -\delta_i & \text{if } [\mathbf{u}_{lin}(\boldsymbol{\zeta})]_i < -\delta_i; \\ [\mathbf{u}_{lin}(\boldsymbol{\zeta})]_i & \text{if } |[\mathbf{u}_{lin}(\boldsymbol{\zeta})]_i| \leq \delta_i; \\ +\delta_i & \text{if } [\mathbf{u}_{lin}(\boldsymbol{\zeta})]_i > \delta_i. \end{cases} \tag{4.1}$$

where $\mathbf{u}_{lin}(\boldsymbol{\zeta}) = -\mathbf{K}(\boldsymbol{\zeta} - \boldsymbol{\zeta}^*)$ and $\mathbf{K}$ must be such that the eigenvalues of $(\mathbf{A} - \mathbf{BK})$ must remain within the unit circle just like in the original OGY method explained in Section 2.5.

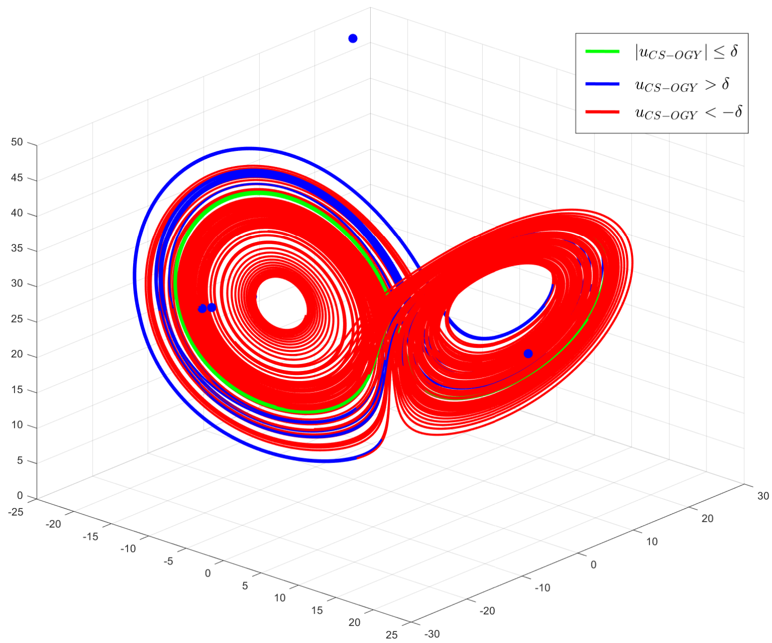

Figure 4.1. CS-OGY sections of the Lorenz attractor for different initial conditions

Let us consider for the sake of simplicity, a chaotic system with single control parameter such that the control input is scalar. The CS-OGY control law divides the state space into three regions: in a narrow region around the target UPO, where the linear control law is applied while the rest of the strange attractor is split into two regions where u is $+\delta$ or $-\delta$, respectively. These regions are shown in Figure 4.1, where the UPO, the $+\delta$ region and the $-\delta$ region are colored with green, blue and red, respectively.

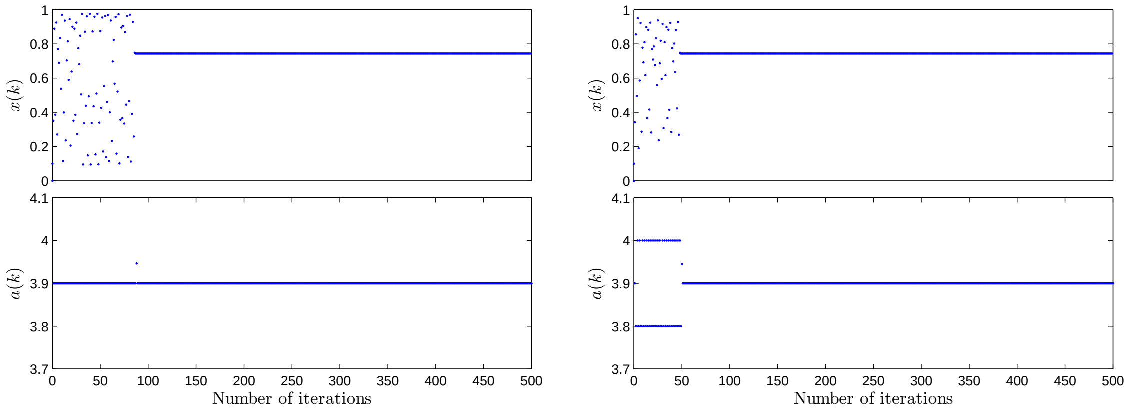

(a) Basic OGY (b) CS-OGY

Figure 4.2. States and control parameter variations of a Logistic map with $a_{nom} = 1.37$ stabilized at $x^* = 0.744$ by (a) basic OGY with $R_{OGY} = 0.01$, and (b) CS-OGY with $|\Delta a| < 0.1$

Figures 4.2 and 4.3 show the states and control parameter changes under the application of (a) the basic OGY control (b) CS-OGY control applied to the Logistic and Henon maps respectively. the depicted simulation results may create the impression that CS-OGY achieves the stabilization of the target faster than the basic OGY control, but this just a coincidence that depends on the initial condition as well as the R_{OGY} in the basic OGY method.

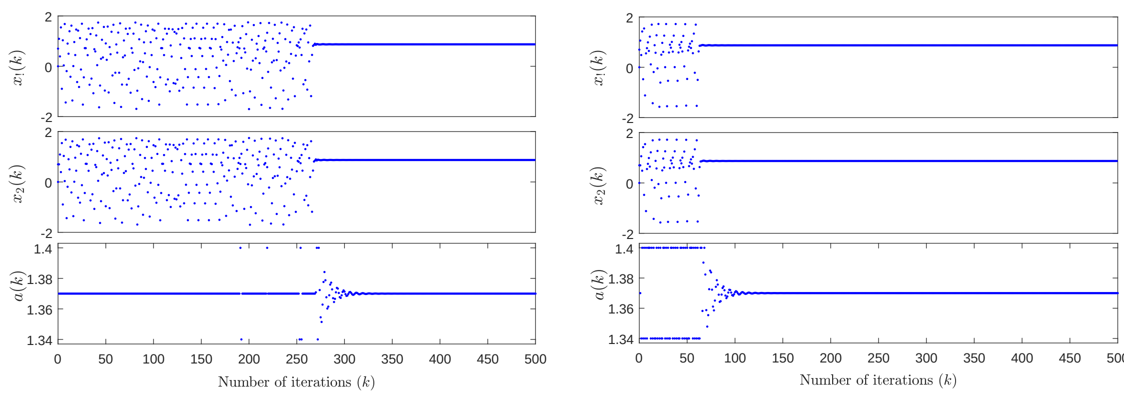

(a) Basic OGY (b) CS-OGY

Figure 4.3. States and control parameter variations of a Henon map with $(a_{nom}, b_{nom}) = (1.37, 0.3)$ stabilized at $\mathbf{w}^* = [0.877, 0.877]^\top$ by (a)basic OGY with $R_{\mathrm{OGY}} = 0.2$, and (b)CS-OGY with $|\Delta a| < 0.03$

4.2. Selective Coupling Strategy

In the network literature, different selective coupling strategies are employed, most of which are based on the spatial proximity of the nodes in the network. Here, a selective coupling criterion is suggested that is based on the similarity of the control effort between any pair of systems in a network.The strategy is dubbed as *Control-Similarity (CoSim) Based Coupling*. Here, for the sake of simplicity, it will be explained only for a system with a single control parameter, thus, a scalar control variable.

Definition 4.1. *Consider two identical chaotic systems D_i and D_j which are stabilized via CS-OGY method at UPO_i and UPO_j respectively. The control similarity (c_{ij}) of D_i to D_j is a measure of the similarity of D_i's control action (u_i) to D_j's control action (u_j) for a predefined threshold (θ_{CoSim}). The ij^{th} component of the instantaneous control similarity matrix $\mathbf{C}(k)$ is defined as follows:*

$$c_{ij}(k) = \begin{cases} 1 & \textit{if } |u_j(k) - u_i(k)| \leq \theta_{CoSim}; \\ 0 & \textit{otherwise}; \end{cases} \tag{4.2}$$

where $\theta_{CoSim} < \delta$ denotes the control similarity threshold. By definition, $c_{ii}(k) = 1 \quad \forall i, k$. Control similarities within a predefined duration (κ), the so-called memory span, can be used to conclude whether D_i will be coupled to D_j. According to the strategy proposed in this study, $\gamma_{ij}(k)$, the ij^{th} component of the coupling matrix $\mathbf{\Gamma}(k)$ is calculated as

$$\gamma_{ij}(k) = \begin{cases} 1 & \textit{if } \dfrac{\sum\limits_{l=1}^{\kappa} c_{ij}(k-l)\alpha^{l-1}}{\sum\limits_{l=1}^{\kappa} \alpha^{l-1}} < \nu; \\ 0 & \textit{otherwise}; \end{cases} \tag{4.3}$$

where $\alpha \in (0, 1]$ denotes the forgetting factor and ν denotes the threshold for the similarity ratio within the memory span.

For an N-node network, CoSim matrix $\mathbf{C}$, is an $N \times N$ binary matrix. Although according to Equation 4.2 $c_{ij} = c_{ji}$, it should be avoided to assume $\mathbf{C}$ as a symmetric matrix because, the control similarity (c_{ij}) if D_i to D_j is to be updated every time system D_i pierces the Poincaré surface S_p in the specified direction, which may not occur simultaneously with D_j's piercing S_p.

There are four parameters affecting the selective coupling. κ, the *memory span* determines how many past steps are considered in the evaluation of control similarity. The *forgetting factor* $\alpha \in (0, 1]$ is used to provide a geometrically decaying relative weight to past control similarity information. The sum in the denominator is used for normalization purposes. As a special case, $\alpha = 1$ provides an equal weight for all records within the memory span. The *similarity ratio threshold* $\nu \in [0, 1]$ corresponds to the minimum value of the weighted average control similarity within the memory span to allow coupling. The fourth parameter is θ_{CoSim} used in the calculation of instantaneous control similarity. These parameters have to be appropriately chosen in order to allow a reasonable selective coupling performance.

For the sake of simplicity, examples will be provided for a two node network of identical Lorenz systems operating in a chaotic regime.

$$\dot{\mathbf{w}}_{\mathbf{i}} = \begin{pmatrix} \dot{x}_i \\ \dot{y}_i \\ \dot{z}_i \end{pmatrix} = \begin{pmatrix} \sigma(y_i - x_i) \\ \rho\hat{q} - y_i - \hat{q}z_i \\ \hat{q}y_i - \beta z_i \end{pmatrix} \tag{4.4}$$

where $\mathbf{w}_{\mathbf{i}} = [x_i,\, y_i,\, z_i]^\top$. Assuming that the drive subsystem consists of the state variable $x = q$ and the coupling variable μ is calculated as

$$\hat{q} = \mu_i = \frac{\sum\limits_{j=1}^{N} \gamma_{ij} x_j}{\sum\limits_{j=1}^{N} \gamma_{ij}} \qquad i, j = 1, 2 \tag{4.5}$$

Simulations on chaotic networks which consist of identical Lorenz systems are performed in MATLAB using Runge-Kutta 4^{th} order method. The nominal parameter values for the Lorenz system are taken as the most commonly used set that provides a chaotic regime with $\sigma = 10$, $\rho = 28$ and $\beta = 8/3$. The Poincaré surface of section, S_p is selected as $z = 27$ and σ is chosen as the control parameter with $|\Delta\sigma| \leq 0.5$ for the Lorenz system.

In [58], a method to extract UPO's from the Lorenz attractor is proposed and UPOs of first 20 period are analyzed. Three distinct UPOs are extracted as in [58]. In Table 4.1, characteristics of the selected UPOs are listed and they are visualized in Figure 4.4.

Table 4.1. Characteristics of the target UPOs used in the simulations

	$\boldsymbol{\zeta^*}$	**K**	**Period (n)**	**Period (sec)**
$\mathbf{UPO_1}$	$[-13.7636, -19.5788, 27]^\top$	[1.16976, 3.1543]	2	1.5587
$\mathbf{UPO_2}$	$[-12.5951, -16.9705, 27]^\top$	[2.15211, 6.0490]	3	2.3059
$\mathbf{UPO_3}$	$[\ 12.5951,\ 16.9705, 27]^\top$	[-2.4021,-6.5977]	3	2.3059

The effects of the parameters κ, α, ν and θ_{CoSim} are shown in Figure 4.5 to 4.8. The simulation results reveal that increasing κ renders coupling/decoupling transitions more difficult, increasing α renders the coupling less sensitive to instantaneous fluctuations in control similarity, increasing ν makes coupling more difficult and increasing θ_{CoSim} makes it easier.

In the rest of this thesis the parameter values will be use as $\kappa = 5$, $\alpha = 1$, $\nu = 0.5$, $\theta_{CoSim} = 0.001 \times \delta$ where $\delta = 0.5$.

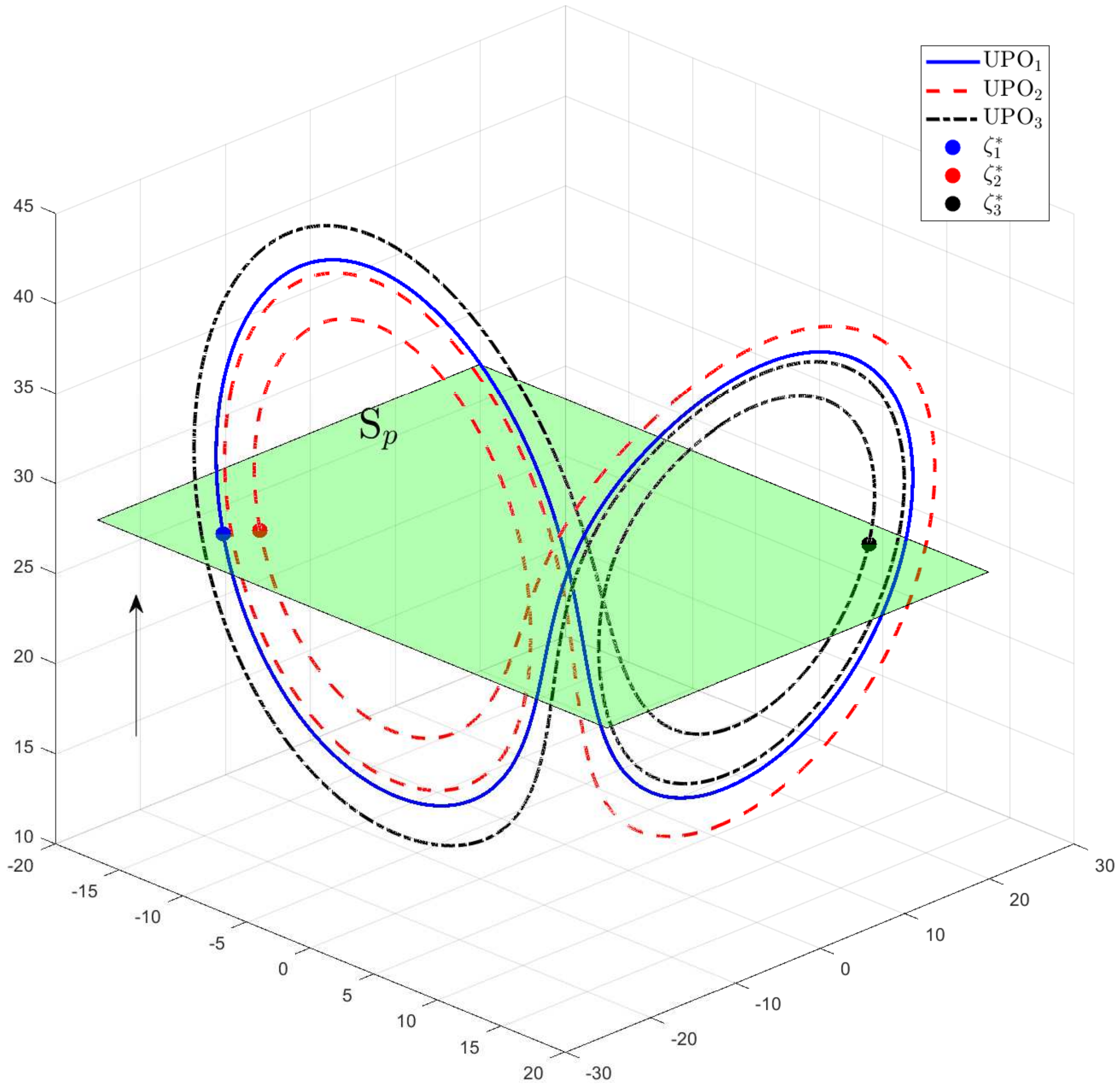

Figure 4.4. Stabilized UPOs of the Lorenz system

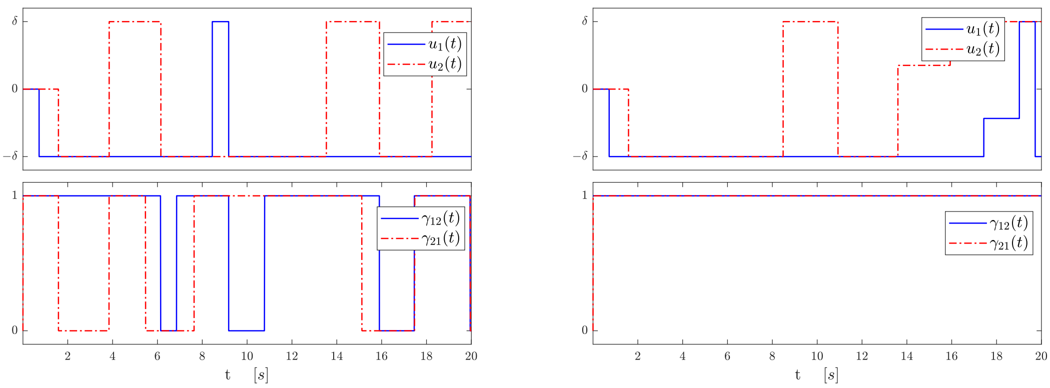

(a) $\kappa = 3$ (b) $\kappa = 20$

Figure 4.5. The control inputs (u_1, u_2) and the coupling statuses (γ_{12}, γ_{21}) of two CS-OGY controlled systems stabilized at UPO_1 and UPO_2 under CoSim-based coupling with $\alpha = 1$, $\nu = 0.5$, $\theta_{CoSim} = \delta \times 10^{-3}$ and (a) $\kappa = 3$, (b) $\kappa = 20$

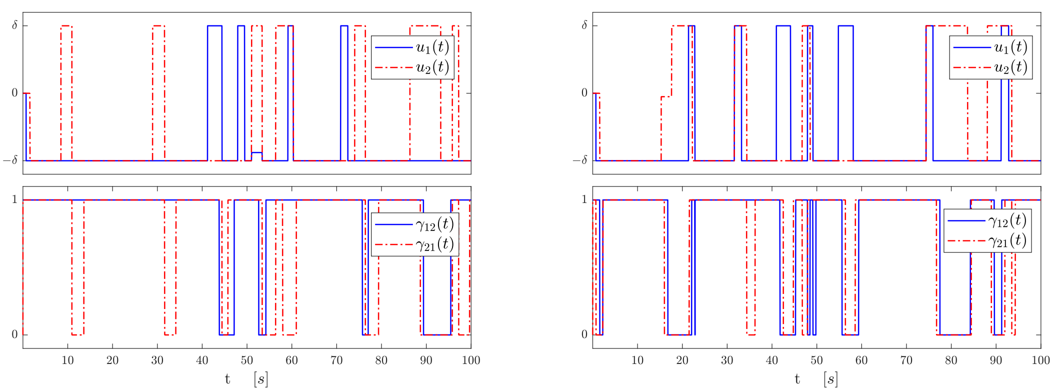

(a) $\alpha = 1$ (b) $\alpha = 0.3$

Figure 4.6. The control inputs (u_1, u_2) and the coupling statuses (γ_{12}, γ_{21}) of two CS-OGY controlled systems stabilized at UPO_1 and UPO_2 under CoSim-based coupling with $\kappa = 5$, $\nu = 0.5$ $\theta_{CoSim} = \delta \times 10^{-3}$ and (a) $\alpha = 1$, (b) $\alpha = 0.3$

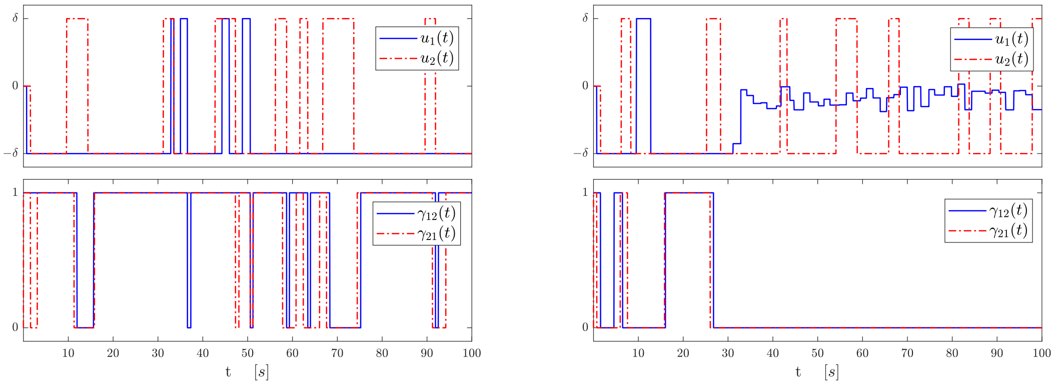

(a) $\nu = 0.5$ (b) $\nu = 0.9$

Figure 4.7. The control inputs (u_1, u_2) and the coupling statuses (γ_{12}, γ_{21}) of two CS-OGY controlled systems stabilized at UPO_1 and UPO_2 under CoSim-based coupling with $\kappa = 6$, $\alpha = 0.7$, $\theta_{CoSim} = \delta \times 10^{-3}$ and (a) $\nu = 0.5$, (b) $\nu = 0.9$

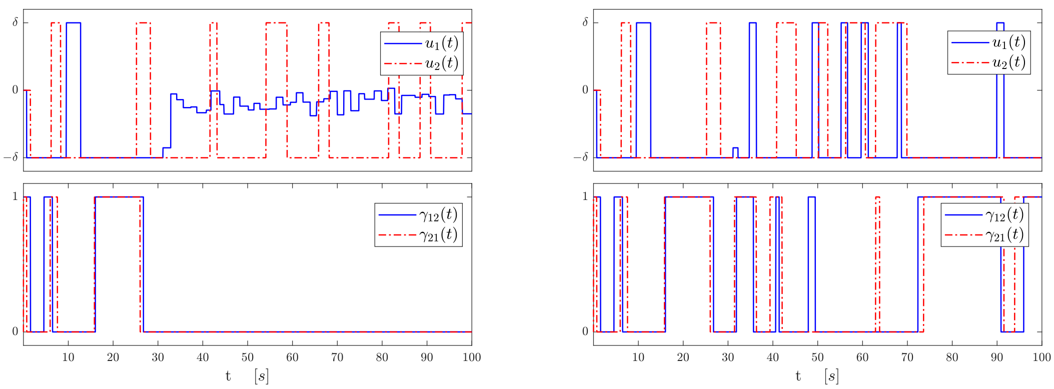

(a) $\theta_{CoSim} = 0.001 \times \delta$ (b) $\theta_{CoSim} = 0.5 \times \delta$

Figure 4.8. The control inputs (u_1, u_2) and the coupling statuses (γ_{12}, γ_{21}) of two CS-OGY controlled systems stabilized at UPO_1 and UPO_2 under CoSim-based coupling with $\kappa = 6$, $\alpha = 0.7$, $\nu = 0.9$ and (a) $\theta_{CoSim} = 0.001 \times \delta$ (b), $\theta_{CoSim} = 0.5 \times \delta$

5. CS-OGY COMBINED WITH DECOMPOSITION BASED SYNCHRONIZATION

The main purpose of the study is to investigate a setup that combines synchronization and OGY control are active in a network of identical chaotic systems. In the previous sections, a modification to the basic OGY method, CS-OGY, has been presented, as well as a control- similarity (CoSim) based coupling strategy for usage with CS-OGY control. In this section possible scenarios will be investigated how CS-OGY control and decomposition based synchronization can interact when the chaotic systems are coupled according to the CoSim based strategy.

Here, for the sake of simplicity, it will be assumed that the CS-OGY control involves only a single control parameter, which is confined to an interval of width 2δ about the nominal value. δ is taken small enough such that even if the CS-OGY control produces a saturated control input ($u = \delta$ or $u = -\delta$) the result is only a slight modification in the strange attractor and the system behavior on it. Consequently, the main characteristics of behavior under OGY control remains unaltered. With a single control parameter, the CS-OGY control results in three different modes of behavior: (i) periodic behavior on the stabilized target UPO, (ii) chaotic behavior on the strange attractor with maximum saturation, (iii) chaotic behavior on the strange attractor with minimum saturation. Thus, if the control similarity threshold is chosen $\theta_{CoSim} << \delta$, a set of two identical chaotic systems controlled by CS-OGY with distinct target UPOs can be found in one of four basic regimes at a given time, except for short transition periods.

5.1. Different Regimes for Two Chaotic Systems

5.1.1. Nonsynchronized Chaotic Motion

The two systems are found in this regime when no coupling is established between them and both are far from their own target UPOs such that they move independently on the strange attractor, sometimes at the maximum, sometimes at the minimum saturation.

The two systems can leave this regime in two different ways depending on whether the stabilization of a target UPO or coupling steps in first.

If at least one of the systems passes close to its own target UPO and is stabilized there, control similarity and thus, coupling will be lost soon. Sooner or later also the other system will be stabilized at its own target UPO such that both systems end up exhibiting independent periodic motion on their own UPOs.

If, on the other hand, two systems moving on the strange attractor happen to be at the same saturation status long enough to satisfy the coupling criterion, most probably, first unidirectional then bidirectional coupling will be established, and soon the systems will start exhibiting synchronized chaotic behavior.

5.1.2. Synchronized Chaotic Motion

As described above, this regime is established when the two systems moving on the strange attractor can remain coupled long enough. As long as there exists sufficient control similarity (weighted average of control similarity during a predefined memory span) the two systems will move in a synchronized manner on the strange attractor. This regime can end due to loss of control similarity and the resulting decoupling, which can step in either because of the two systems happen to be in opposite control saturation status or because they pass close to their target UPOs.

5.1.3. Chaotic and Periodic Motions

This regime corresponds to the case, where one of the systems is moving on the strange attractor, while the other is stabilized at its own target UPO. This regime will end when the system moving on the strange attractor eventually comes close to its target UPO and stabilized there.

5.1.4. Independent Periodic Motion

This is the regime where the two systems move on their own target UPOs. The establishment of control similarity is very improbable in case of distinct target UPOs such that this regime will be maintained indefinitely, unless an external disturbance intervenes. As a special case, if the systems happen to have identical target UPOs, the coupling criterion may be satisfied leading to synchronized periodic motion.

If there exists systems with the same target UPO, a special steady state behavior of *synchronized periodic motion* on the UPO will be achieved.

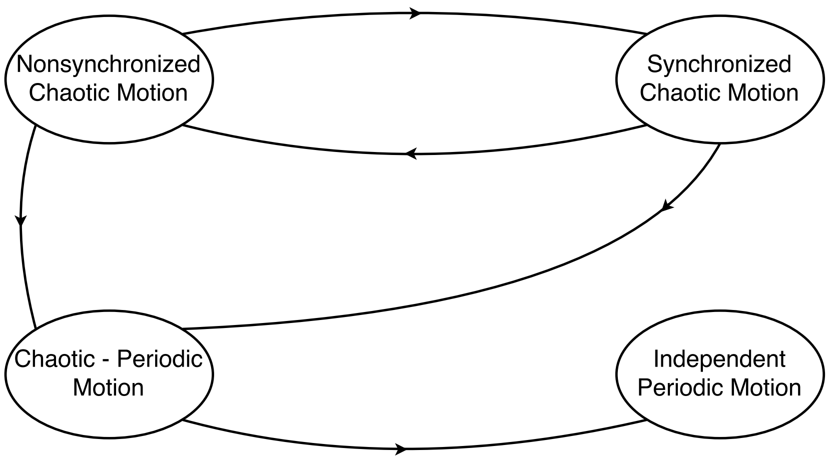

Figure 5.1. Different regimes for two identical chaotic systems under CoSim-based coupling CS-OGY control with distinct target UPOs

When and which of the transitions between these regimes will occur depends on the values of the parameters of the selective coupling scheme (memory span (κ), forgetting factor (α), similarity ratio threshold (ν) and control similarity threshold (θ_{CoSim})), as well as on the exact states of the individual systems. Longer memory span (κ) values render regime transitions more difficult because the inertia of the past, weights out changes in the instantaneous control similarity. This effect of long memory span can be compensated by choosing smaller forgetting factor (α) and a higher similarity ratio threshold (ν). Therefore, κ, α and ν have to be adjusted simultaneously to suitable values to achieve reasonable transition probabilities between the regimes. The control similarity threshold (θ_{CoSim}) needs to be chosen $<< \delta$, such that coupling is favored only between systems in chaotic mode with the same control saturation.

As stated before and can be seen in Figure 5.1, for two identical chaotic systems under CoSim-based coupling and CS-OGY control with distinct target UPOs, independent periodic behavior of each system on its own target UPO is the ultimate regime, which will be maintained unless an external disturbance destabilizes their periodic behavior.

Figure 5.2 shows the transitions for a two node network for $\kappa = 5$, $\alpha = 1$, $\nu = 0.5$ and $\theta_{CoSim} = 0.001 \times \delta$.

5.2. The Effect of Disturbance

CS-OGY, just like the original OGY method, uses a control law that is derived from an approximate local model of the system dynamics within a close neighborhood of the target UPO. If there is some disturbance on the system dynamics such as a change in a parameter value or some additive noise, this may lead to a situation where the control law fails to stabilize the target UPO and the system will enter chaotic mode. Based on this idea, if a large (but not large enough to change the chaotic dynamics) disturbance is applied in the same manner to both systems moving independently on their distinct UPOs, both systems are expected to leave periodic motion and start chaotic motion on the strange attractor.

It should be noted that, there will be some distortion in the strange attractor due to the disturbed system dynamics, but this distortion will be the same for both systems.

When the control signals of both systems remain large enough at the same saturation mode, coupling will be established and eventually the systems will exhibit synchronized chaotic motion. However, the synchronized chaotic motion under common disturbance differs from the synchronized chaotic motion under undisturbed conditions in respect: as long as the disturbance persists the systems cannot revert to periodic motion because CS-OGY control fails to fulfill stabilizing task under disturbed conditions. Nevertheless, the two systems, now and then, may loose and regain CoSim based coupling and thus, synchronicity. When the disturbance is removed, regime transitions as described in Section 5.1 will again be possible.

In Figure 5.3, effect of common disturbance to a two node network is shown for $\kappa = 5$, $\alpha = 1$, $\nu = 0.5$ and $\theta_{CoSim} = 0.001 \times \delta$.

5.3. Multi-Node Networks

As the number of nodes in the network increases, systems' tendency will evolve on the advantage of synchronization since there will be more choice of coupling. Taking into consideration that each coupling effort (even tough it is not persistent), interrupts the OGY control procedure by deforming the attractor with the dynamics of coupling. Sooner or later this, CS-OGY control will succeed to overcome this deformation at the intervals with loose coupling. In that sense, it can be concluded that if the number of nodes in the network increases, selective coupling parameters shall be tuned in a way that allow weaker coupling. Otherwise, synchronization will not allow stabilization to be achieved.

In Figure 5.4, transitions for a three node network is shown for $\kappa =$, $\alpha =$, $\nu =$ and $\theta_{CoSim} = 0.001 \times \delta$. In Figure 5.5, transitions for a four node network is shown for $\kappa =$, $\alpha =$, $\nu =$ and $\theta_{CoSim} = 0.001 \times \delta$.

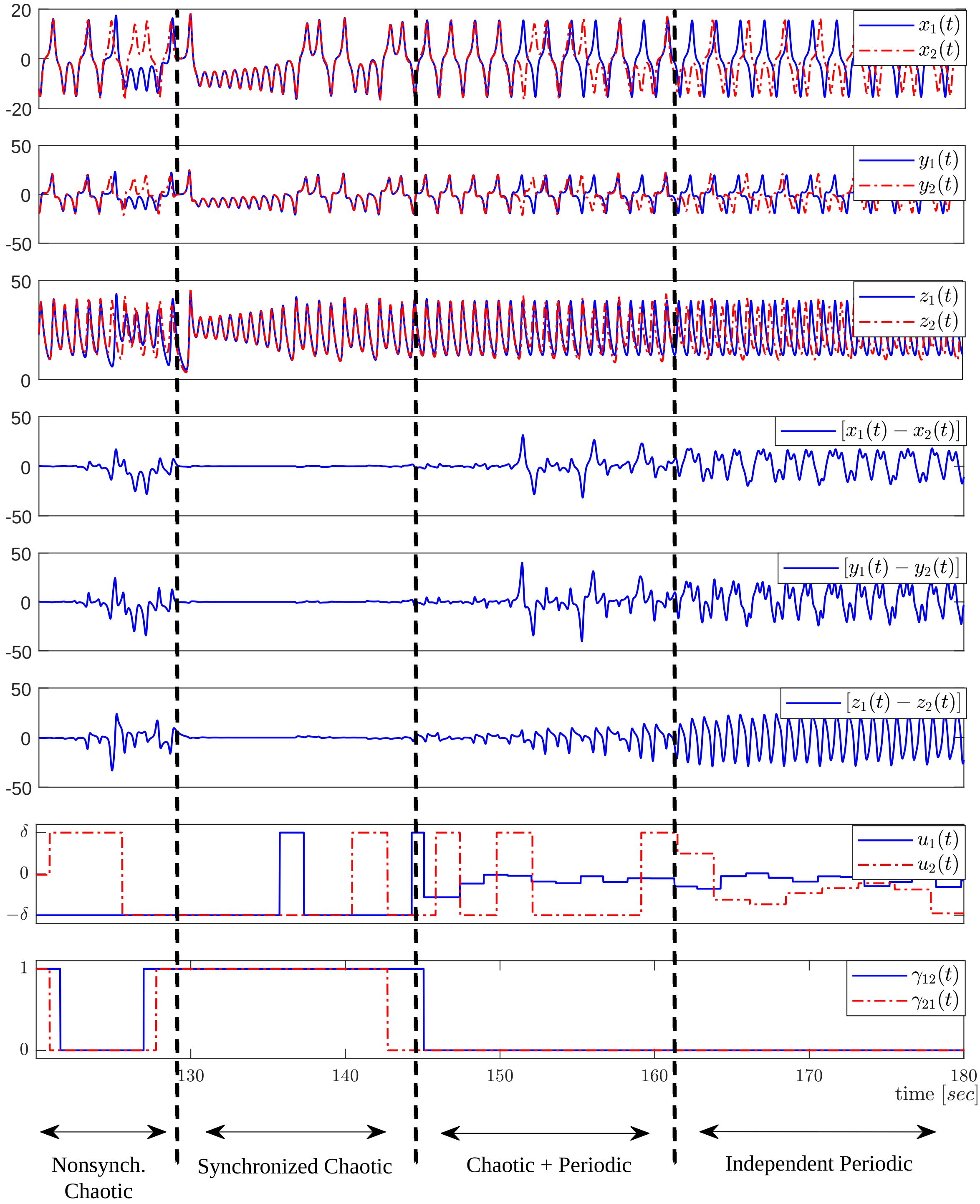

Figure 5.2. Transitions between different regimes in a two-node network consisting of two chaotic systems under CoSim-based coupling and CS-OGY control with target UPO_1 and UPO_2 respectively.

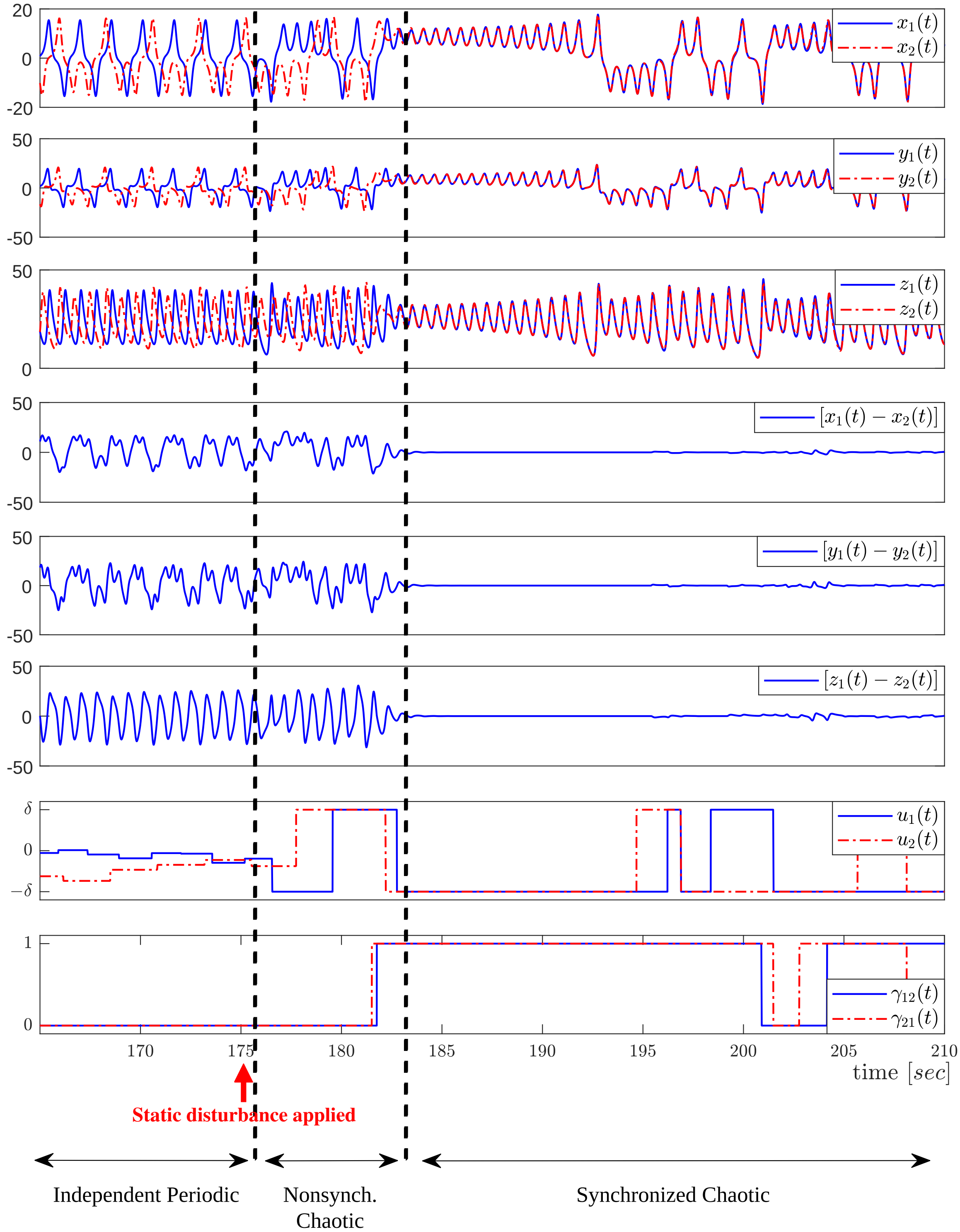

Figure 5.3. Effect of common disturbance in a two node network (β is increased from 8/3 to 3 at 175 sec.)

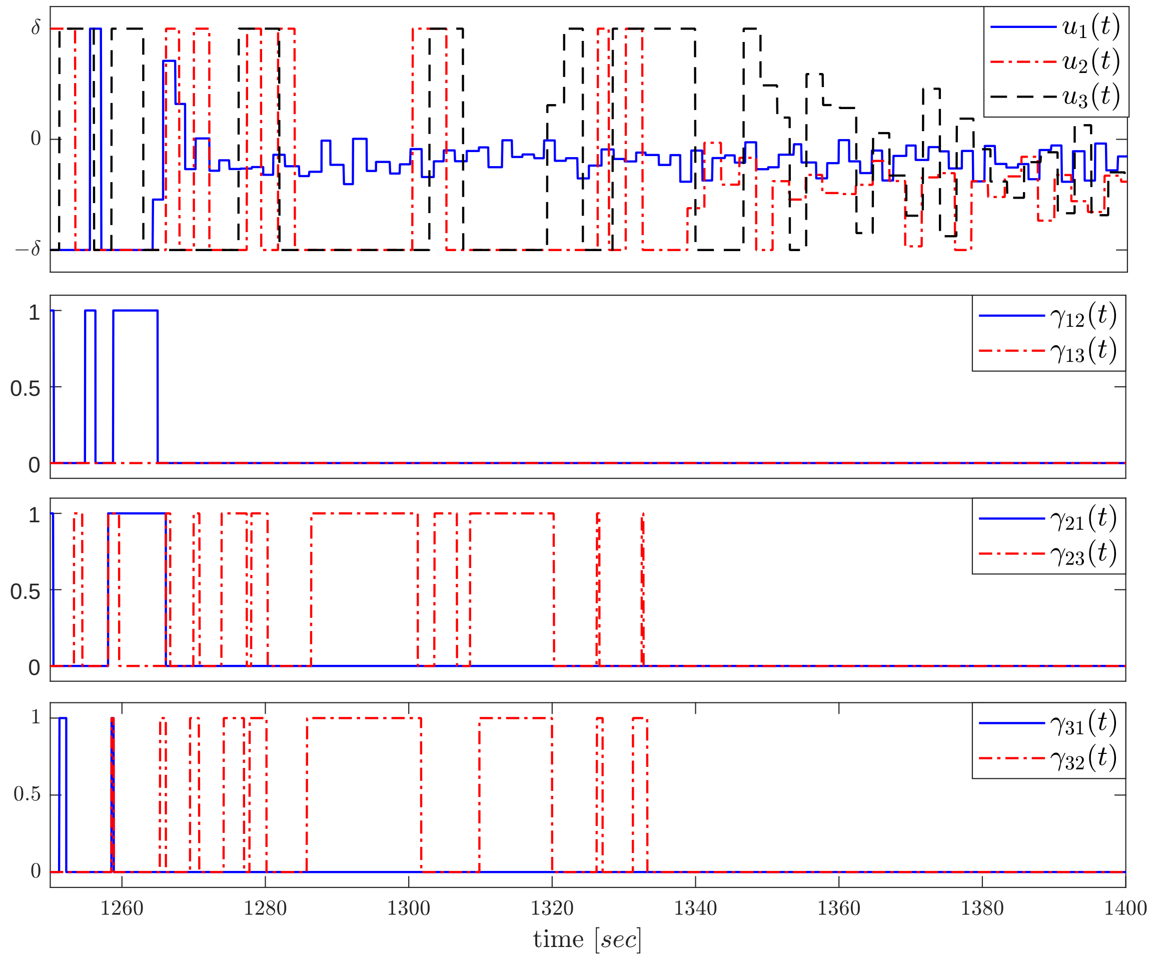

Figure 5.4. Transitions between different regimes in a three-node network consisting of three chaotic systems under CoSim-based coupling and CS-OGY control with target UPO_1, UPO_2 and UPO_3 respectively.

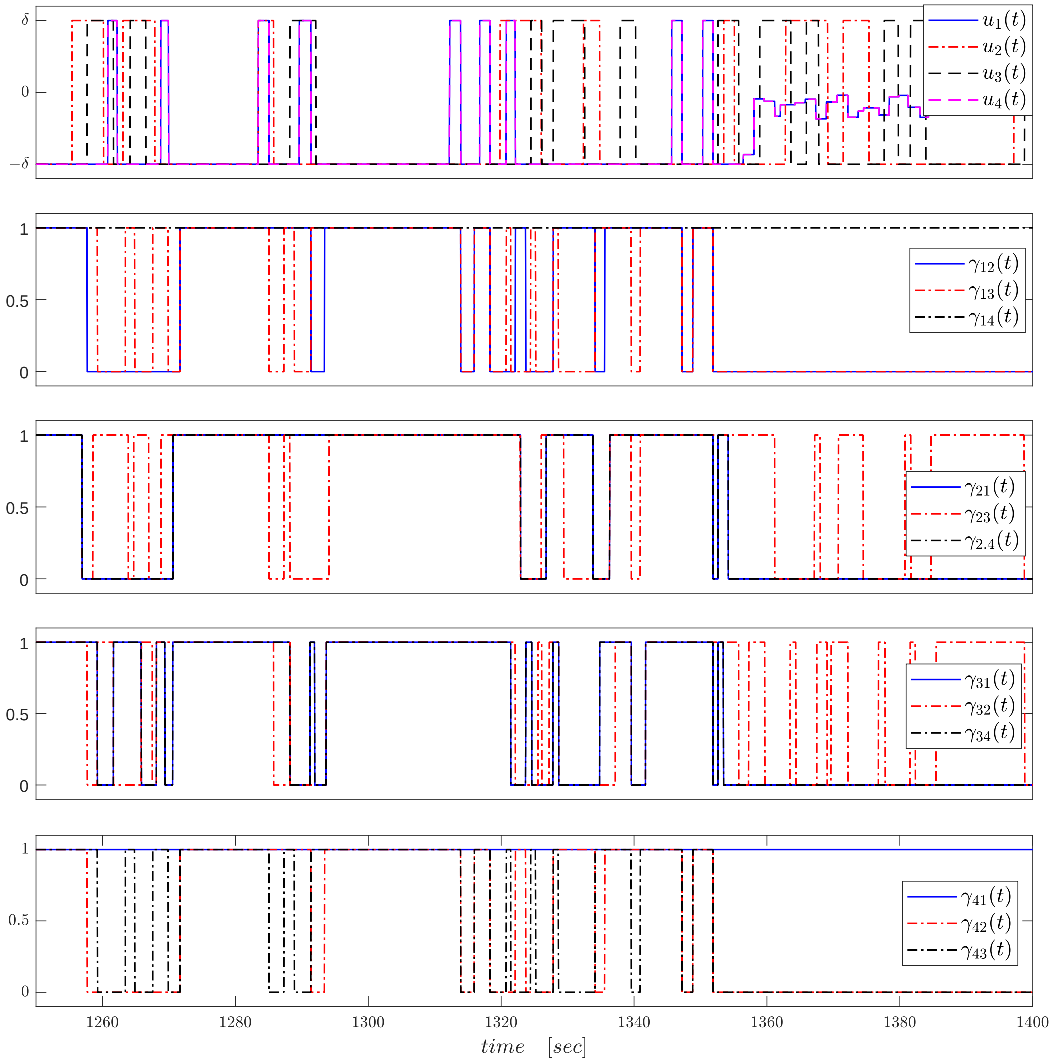

Figure 5.5. Transitions between different regimes in a four-node network consisting of four chaotic systems under CoSim-based coupling and CS-OGY control with target UPO_1, UPO_2, UPO_3 and UPO_1 respectively.

6. CONCLUSION

In this thesis, competition between control and synchronization have been investigated in networks consisting of a few chaotic systems. For this purpose, a slightly modified version of the original OGY control dubbed control-saturated OGY (CS-OGY) method and an original coupling strategy dubbed control-similarity based coupling have been developed. The coupling component is selected according to the decomposition based synchronization method, which decomposes each of the chaotic systems to be coupled into two subsystems, a drive and a response subsystem, where the response subsystem has to be stable. Among all investigated coupling configurations, autonomous mean field replacement of the coupling component has been chosen as the most adequate one due to its robust characteristics in numerical results and having analytical stability solution to the examined Lorenz system. An original coupling criterion is introduced, based on the control similarity of the chaotic systems in the network.

The combination of the control and synchronization methods via CoSim based coupling has been simulated on 2, 3 and 4 node networks consisting of Lorenz systems, CS-OGY stabilized at distinct UPOs. The original contributions and findings of this thesis can be summarized as follows.

6.1. Novel Synchronization Scheme

Complete synchronization of chaotic systems coupled according to the decomposition based synchronization approach has been investigated for various coupling configurations, and *bidirectional mean-field replacement* of the coupling component has been found as the configuration that guarantees complete synchronization. This specific form of coupling has not been investigated previously in the chaos synchronization literature. The stability of synchronization achieved with such coupling scheme has been both proven analytically and demonstrated via simulation results obtained for coupled Lorenz systems. Also, *unidirectional mean-field replacement* of the coupling component is shown to be stable for Lorenz systems in the numerical simulations.

6.2. Novel Modification of the OGY Method

Classical OGY method is designed to be activated only within a small region around the target UPO such that the corresponding control law is defined in a piecewise manner and results in a discontinuity of the control action. The suggested *CS-OGY method*, however, does not confine the control activity to a specific state-space region. Instead, the control action is saturated when its magnitude reaches a predefined value. Thus, the control action within a close neighborhood of the target UPO is identical to that of the classical OGY control, while outside this neighborhood the control activity switches between the maximum and minimum saturation values. This behavior far from the target UPO can per se be disadvantageous in the sense that it may alter the characteristic chaotic motion on the strange attractor, which guarantees that the system state will sooner or later pass close to the target UPO. Nevertheless, for sufficiently small saturation threshold no such effect is observed.

Successful implementation results of the proposed CS-OGY method are given for the Logistic map, the Henon map and the Lorenz system employing only a single control parameter.

Implementation of the CS-OGY method to the other benchmark chaotic systems and hyper chaotic systems and usage of multiple control parameters are left as a future work.

6.3. Control-Similarity Based Coupling

If identical chaotic systems which are stabilized at distinct target UPOs via OGY or CS-OGY control, are bidirectionally mean-field coupled, synchronization supersedes control such that the systems soon leave the stabilized UPOs and synchronize on the strange attractor. To make the competition between the control and synchronization tendencies nontrivial, a selective coupling scheme has been developed that is based on the similarity of the control actions of different chaotic systems. Four parameters, (i) control similarity threshold, (ii) memory span, (iii) forgetting factor and (iv) similarity ratio threshold are critical for the performance of such a coupling scheme. With a reasonable choice of the involved parameters, the control-similarity-based coupling scheme allows interesting scenarios to be observed between the regimes of independent periodic motion and synchronized chaotic motion.

6.4. Competition between Control and Synchronization

When two identical chaotic systems are stabilized via CS-OGY at distinct UPOs are mean-field coupled according to the CoSim based coupling strategy, these system can go through a number of different regimes: *independent chaotic motion*, *synchronized chaotic motion*, *one system periodic-the other system chaotic*, *independent periodic motion*. Depending on the initial conditions, two systems network can start from any of these regimes, but in the long run the most stable regime is the independent periodic motion of the two systems on their distinct target UPOs.

If several identical chaotic systems with various (possibly also identical) target UPOs are coupled in a similar manner the number of combinations increases, nevertheless, the most stable regime is when systems with identical target UPOs form clusters exhibiting synchronized periodic behavior, while clusters corresponding to distinct UPOs exhibit periodic motion independent of each other.

6.5. Effect of Common Disturbance

Let us imagine that all chaotic systems in a network are exposed to the same static disturbance which is large enough to render obsolete the CS-OGY control law that is based on undisturbed system model, but small enough to preserve chaotic nature of the system dynamics. Under this scenario, the CS-OGY controllers will no more be able to stabilize their target UPOs and therefore, all systems will start exhibiting chaotic motion, and - as long as the static disturbance persists - will be unable to return to the periodic behavior. Furthermore, while traveling on the (slightly shifted) strange attractors, the systems may attain control similarity, be coupled and start exhibiting synchronized chaotic motion. However, the stability of such coupling and synchronized chaotic motion depends on how compatible their target UPOs are because it is this compatibility that determines whether they will be in the same saturation modes (i.e. minimum or maximum) while moving in a synchronized manner. To give the most extreme case, if two systems have target UPOs that are the mirror image of each with respect to a reflection (hyper) plane, their control activities will be mostly in opposite saturation modes such that CoSim coupling will never be established. If the chaotic systems have moderately compatible target UPOs, the most stable regime under (moderate) static disturbance is synchronized chaotic regime. Upon removal of the disturbance, independent periodic motion on distinct UPOs again becomes the most stable regime.

6.6. Conclusion

With an appropriate choice of parameters, the combination of OGY control and synchronization through control-similarity based coupling provides different dynamic regimes and meaningful transitions between them. As such, it can serve as a good model for different types of collective behavior at various organizational levels, particularly in living systems in particular.

This thesis provides a proof of the concept for this combination through a MATLAB based simulation of small sized networks consisting of identical Lorenz systems. This novel idea harbors many details that need to be investigated and expanded. Some basic issues that ask for further research are the development of heuristics for choosing the parameter values, elaboration of the case with multiple control parameters and implementations on other benchmark systems as well as on larger networks.

REFERENCES

1. Lorenz, E. N., "Deterministic nonperiodic flow", *Journal of the atmospheric sciences*, Vol. 20, No. 2, pp. 130–141, 1963.

2. Li, T.-Y. and J. A. Yorke, "Period three implies chaos", *The American Mathematical Monthly*, Vol. 82, No. 10, pp. 985–992, 1975.

3. May, R. M. *et al.*, "Simple mathematical models with very complicated dynamics", *Nature*, Vol. 261, No. 5560, pp. 459–467, 1976.

4. Hénon, M., "A two-dimensional mapping with a strange attractor", *The Theory of Chaotic Attractors*, pp. 94–102, Springer, 1976.

5. Rössler, O. E., "An equation for continuous chaos", *Physics Letters A*, Vol. 57, No. 5, pp. 397–398, 1976.

6. Chua, L. O., C. W. Wu, A. Huang and G.-Q. Zhong, "A universal circuit for studying and generating chaos. I. Routes to chaos", *IEEE Transactions on Circuits and Systems I: Fundamental Theory and Applications*, Vol. 40, No. 10, pp. 732–744, 1993.

7. Ott, E., C. Grebogi and J. A. Yorke, "Controlling chaos", *Physical review letters*, Vol. 64, No. 11, p. 1196, 1990.

8. Ditto, W. L., S. N. Rauseo and M. L. Spano, "Experimental control of chaos", *Physical Review Letters*, Vol. 65, No. 26, p. 3211, 1990.

9. Akhmet, M. and M. O. Fen, "Chaotic period-doubling and OGY control for the forced Duffing equation", *Communications in Nonlinear Science and Numerical Simulation*, Vol. 17, No. 4, pp. 1929–1946, 2012.

10. Peng, B., V. Petrov and K. Showalter, "Controlling chemical chaos", *The Journal of Physical Chemistry*, Vol. 95, No. 13, pp. 4957–4959, 1991.

11. Bueno, R. S. and J. L. R. Marrero, "Application of the OGY method to the control of chaotic DC-DC converters: Theory and experiments", *Circuits and Systems, 2000. Proceedings. ISCAS 2000 Geneva. The 2000 IEEE International Symposium on*, Vol. 2, pp. 369–372, IEEE, 2000.

12. Dressler, U. and G. Nitsche, "Controlling chaos using time delay coordinates", *Physical Review Letters*, Vol. 68, No. 1, p. 1, 1992.

13. Nitsche, G. and U. Dressler, "Controlling chaotic dynamical systems using time delay coordinates", *Physica D: Nonlinear Phenomena*, Vol. 58, No. 1-4, pp. 153–164, 1992.

14. Ritz, T., A. S. Zu Chweinsberg, U. Dressler, R. Doerner, B. Hübinger and W. Martienssen, "Chaos control with adjustable control times", *Chaos, Solitons & Fractals*, Vol. 8, No. 9, pp. 1559–1576, 1997.

15. de Paula, A. S. and M. A. Savi, "A multiparameter chaos control method based on OGY approach", *Chaos, Solitons & Fractals*, Vol. 40, No. 3, pp. 1376–1390, 2009.

16. Romeiras, F. J., C. Grebogi, E. Ott and W. Dayawansa, "Controlling chaotic dynamical systems", *Physica D: Nonlinear Phenomena*, Vol. 58, No. 1-4, pp. 165–192, 1992.

17. Barreto, E. and C. Grebogi, "Multiparameter control of chaos", *Physical Review E*, Vol. 52, No. 4, p. 3553, 1995.

18. Garfinkel, A., "Controlling cardiac chaos", *Science*, 1992.

19. Pyragas, K., "Continuous control of chaos by self-controlling feedback", *Physics letters A*, Vol. 170, No. 6, pp. 421–428, 1992.

20. Konishi, K. and H. Kokame, "Learning control of time-delay chaotic systems and its applications", *International Journal of Bifurcation and Chaos*, Vol. 8, No. 12, pp. 2457–2465, 1998.

21. Ushio, T. and S. Yamamoto, "Delayed feedback control with nonlinear estimation in chaotic discrete-time systems", *Physics Letters A*, Vol. 247, No. 1-2, pp. 112–118, 1998.

22. Yamamoto, S., T. Hino and T. Ushio, "Dynamic delayed feedback controllers for chaotic discrete-time systems", *IEEE Transactions on Circuits and Systems I: Fundamental Theory and Applications*, Vol. 48, No. 6, pp. 785–789, 2001.

23. Zeng, Y. and S. N. Singh, "Adaptive control of chaos in Lorenz system", *Dynamics and control*, Vol. 7, No. 2, pp. 143–154, 1997.

24. Liao, T.-L. and S.-H. Lin, "Adaptive control and synchronization of Lorenz systems", *Journal of the Franklin Institute*, Vol. 336, No. 6, pp. 925–937, 1999.

25. Chen, S. and J. Lü, "Synchronization of an uncertain unified chaotic system via adaptive control", *Chaos, Solitons & Fractals*, Vol. 14, No. 4, pp. 643–647, 2002.

26. Feki, M., "An adaptive chaos synchronization scheme applied to secure communication", *Chaos, Solitons & Fractals*, Vol. 18, No. 1, pp. 141–148, 2003.

27. Yassen, M., "Adaptive chaos control and synchronization for uncertain new chaotic dynamical system", *Physics Letters A*, Vol. 350, No. 1, pp. 36–43, 2006.

28. Boccaletti, S., A. Farini and F. Arecchi, "Adaptive synchronization of chaos for secure communication", *Physical Review E*, Vol. 55, No. 5, p. 4979, 1997.

29. Boccaletti, S. and F. Arecchi, "Adaptive control of chaos", *EPL (Europhysics Letters)*, Vol. 31, No. 3, p. 127, 1995.

30. Tanaka, K., T. Ikeda and H. O. Wang, "A unified approach to controlling chaos via

an LMI-based fuzzy control system design", *IEEE Transactions on Circuits and Systems I: Fundamental Theory and Applications*, Vol. 45, No. 10, pp. 1021–1040, 1998.

31. Wang, H. O., K. Tanaka and T. Ikeda, "Fuzzy modeling and control of chaotic systems", *Circuits and Systems, 1996. ISCAS'96., Connecting the World., 1996 IEEE International Symposium on*, Vol. 3, pp. 209–212, IEEE, 1996.

32. Calvo, O. and J. H. Cartwright, "Fuzzy control of chaos", *International Journal of Bifurcation and Chaos*, Vol. 8, No. 08, pp. 1743–1747, 1998.

33. Wang, H. O. and K. Tanaka, "An LMI-based stable fuzzy control of nonlinear systems and its application to control of chaos", *Fuzzy Systems, 1996., Proceedings of the Fifth IEEE International Conference on*, Vol. 2, pp. 1433–1438, IEEE, 1996.

34. Lin, C.-T. and C.-P. Jou, "Controlling chaos by GA-based reinforcement learning neural network", *IEEE Transactions on Neural Networks*, Vol. 10, No. 4, pp. 846–859, 1999.

35. Zhou, S., H. Li and Z. Zhu, "Chaos control and synchronization in a fractional neuron network system", *Chaos, Solitons & Fractals*, Vol. 36, No. 4, pp. 973–984, 2008.

36. Pecora, L. M. and T. L. Carroll, "Synchronization in chaotic systems", *Physical review letters*, Vol. 64, No. 8, p. 821, 1990.

37. Cuomo, K. M. and A. V. Oppenheim, "Circuit implementation of synchronized chaos with applications to communications", *Physical review letters*, Vol. 71, No. 1, p. 65, 1993.

38. Barahona, M. and L. M. Pecora, "Synchronization in small-world systems", *Physical review letters*, Vol. 89, No. 5, p. 054101, 2002.

39. Lü, J., T. Zhou and S. Zhang, "Chaos synchronization between linearly coupled chaotic systems", *Chaos, Solitons & Fractals*, Vol. 14, No. 4, pp. 529–541, 2002.

40. Rulkov, N. F., M. M. Sushchik, L. S. Tsimring and H. D. Abarbanel, "Generalized synchronization of chaos in directionally coupled chaotic systems", *Physical Review E*, Vol. 51, No. 2, p. 980, 1995.

41. Rosenblum, M. G., A. S. Pikovsky and J. Kurths, "Phase synchronization of chaotic oscillators", *Physical review letters*, Vol. 76, No. 11, p. 1804, 1996.

42. Pikovsky, A. S., M. G. Rosenblum, G. V. Osipov and J. Kurths, "Phase synchronization of chaotic oscillators by external driving", *Physica D: Nonlinear Phenomena*, Vol. 104, No. 3-4, pp. 219–238, 1997.

43. Strogatz, S. H., "From Kuramoto to Crawford: exploring the onset of synchronization in populations of coupled oscillators", *Physica D: Nonlinear Phenomena*, Vol. 143, No. 1, pp. 1–20, 2000.

44. Watts, D. J. and S. H. Strogatz, "Collective dynamics of 'small-world'networks", *nature*, Vol. 393, No. 6684, pp. 440–442, 1998.

45. Lü, J., X. Yu and G. Chen, "Chaos synchronization of general complex dynamical networks", *Physica A: Statistical Mechanics and its Applications*, Vol. 334, No. 1, pp. 281–302, 2004.

46. Chen, M., "Chaos synchronization in complex networks", *IEEE Transactions on Circuits and Systems I: Regular Papers*, Vol. 55, No. 5, pp. 1335–1346, 2008.

47. Fujigaki, H. and T. Shimada, "Phase synchronization and nonlinearity decision in the network of chaotic flows", *Physical Review E*, Vol. 55, No. 3, p. 2426, 1997.

48. Fujisaka, H. and T. Yamada, "Stability theory of synchronized motion in coupled-oscillator systems", *Progress of theoretical physics*, Vol. 69, No. 1, pp. 32–47, 1983.

49. Cuomo, K. M., A. V. Oppenheim and S. H. Strogatz, "Synchronization of Lorenz-based chaotic circuits with applications to communications", *IEEE Transactions on circuits and systems II: Analog and digital signal processing*, Vol. 40, No. 10, pp. 626–633, 1993.

50. Pecora, L. M. and T. L. Carroll, "Master stability functions for synchronized coupled systems", *Physical review letters*, Vol. 80, No. 10, p. 2109, 1998.

51. Schöll, E. and H. G. Schuster, *Handbook of chaos control*, John Wiley & Sons, 2008.

52. Shinbrot, T., E. Ott, C. Grebogi and J. A. Yorke, "Using chaos to direct trajectories to targets", *Physical Review Letters*, Vol. 65, No. 26, p. 3215, 1990.

53. Boccaletti, S., A. Farini, E. Kostelich and F. Arecchi, "Adaptive targeting of chaos", *Physical Review E*, Vol. 55, No. 5, p. R4845, 1997.

54. Iplikci, S. and Y. Denizhan, "Control of chaotic systems using targeting by extended control regions method", *Physica D: Nonlinear Phenomena*, Vol. 150, No. 3, pp. 163–176, 2001.

55. Iplikci, S. and Y. Denizhan, "An improved neural network based targeting method for chaotic dynamics", *Chaos, Solitons & Fractals*, Vol. 17, No. 2, pp. 523–529, 2003.

56. Chen, G. and X. Dong, "From chaos to order—perspectives and methodologies in controlling chaotic nonlinear dynamical systems", *International Journal of Bifurcation and Chaos*, Vol. 3, No. 06, pp. 1363–1409, 1993.

57. Chen, G. and X. Yu, *Chaos control: theory and applications*, Vol. 292, Springer Science & Business Media, 2003.

58. Viswanath, D., "Symbolic dynamics and periodic orbits of the Lorenz attractor",

Nonlinearity, Vol. 16, No. 3, p. 1035, 2003.

59. Slotine, J.-J. E., W. Li *et al.*, *Applied nonlinear control*, Vol. 199, prentice-Hall Englewood Cliffs, NJ, 1991.

60. Mainieri, R. and J. Rehacek, “Projective synchronization in three-dimensional chaotic systems”, *Physical Review Letters*, Vol. 82, No. 15, p. 3042, 1999.

61. Li, G.-H., “Modified projective synchronization of chaotic system”, *Chaos, Solitons & Fractals*, Vol. 32, No. 5, pp. 1786–1790, 2007.

62. Du, H., Q. Zeng and C. Wang, “Function projective synchronization of different chaotic systems with uncertain parameters”, *Physics Letters A*, Vol. 372, No. 33, pp. 5402–5410, 2008.

63. Du, H., Q. Zeng and C. Wang, “Modified function projective synchronization of chaotic system”, *Chaos, Solitons & Fractals*, Vol. 42, No. 4, pp. 2399–2404, 2009.

64. Abarbanel, H. D., N. F. Rulkov and M. M. Sushchik, “Generalized synchronization of chaos: The auxiliary system approach”, *Physical Review E*, Vol. 53, No. 5, p. 4528, 1996.

65. Moskalenko, O. I., A. A. Koronovskii, A. E. Hramov and S. Boccaletti, “Generalized synchronization in mutually coupled oscillators and complex networks”, *Physical Review E*, Vol. 86, No. 3, p. 036216, 2012.

66. Rosenblum, M. G., A. S. Pikovsky and J. Kurths, “From phase to lag synchronization in coupled chaotic oscillators”, *Physical Review Letters*, Vol. 78, No. 22, p. 4193, 1997.

67. Shahverdiev, E., S. Sivaprakasam and K. Shore, “Lag synchronization in time-delayed systems”, *Physics Letters A*, Vol. 292, No. 6, pp. 320–324, 2002.

68. Guo, W., “Lag synchronization of complex networks via pinning control”, *Nonlin-*

ear Analysis: Real World Applications, Vol. 12, No. 5, pp. 2579–2585, 2011.

69. Li, G.-H., "Projective lag synchronization in chaotic systems", *Chaos, Solitons & Fractals*, Vol. 41, No. 5, pp. 2630–2634, 2009.

APPENDIX A: STABILITY DEFINITIONS

The following definitions related to continuous-time systems are taken from [59]. Let us consider a dynamic system $\dot{\mathbf{w}}(t) = \mathbf{f}(\mathbf{w}(t))$.

Definition A.1. *An equilibrium point* $\mathbf{w}^*$ *is said to be stable if, for any* $R > 0$, *there exists* $r > 0$, *such that if* $||\mathbf{w}(0)|| < r$, *then* $||\mathbf{w}(t)|| < R$ *for all* $t > 0$ *. Otherwise, the equilibrium point is unstable.*

Definition A.2. *An equilibrium point* $\mathbf{w}*$ *of is asymptotically stable if it is stable, and if in addition there exists some* $r > 0$ *such that* $||\mathbf{w}(0)|| < r$ *implies that for* $\mathbf{w}t) \to 0$ *as* $t \to \infty$.

Definition A.3. *An equilibrium point* $\mathbf{w}*$ *is exponentially stable if there exist two strictly positive numbers* υ *and* λ *such that*

$$\forall t > 0, ||\mathbf{w}(t)|| < \upsilon ||\mathbf{w}(O)|| e^{\lambda t}$$

in some ball B_r *around* $\mathbf{w}^*$.

Definition A.4. *If asymptotic (or exponential) stability holds for any initial states, the equilibrium point is said to be globally asymptotically (or exponentially) stable in the large.*

Theorem A.5. *Consider the linearization of the original nonlinear system in the equilibrium point* $\mathbf{w}^*$ *as*

$$\dot{\mathbf{w}} = \mathbf{A}\mathbf{w}$$

where

$$A = \left(\frac{\partial \mathbf{f}}{\partial \mathbf{w}}\right)$$

Then,

- *if all eigenvalues of A has positive real parts, then* $\mathbf{w}^*$ *is asymptotically stable for the actual nonlinear system.*

- *If the eigenvalues of A has negative real parts, then* $\mathbf{w}^*$ *is unstable*

- *If all of the eigenvalues of A has negative real parts except at least one with zero real part, then no conclusion can be made for* $\mathbf{w}^*$ *of nonlinear systems. If the original system is already linear, then* $\mathbf{w}^* = \mathbf{0}$ *is marginally stable.*

Lyapunov stability related definitions and theorems.

Definition A.6. *A scalar continuous function $V(\mathbf{w})$ is said to be locally positive definite if $V(\mathbf{0}) = 0$ and, in a ball B_R*

$$\mathbf{w} \neq 0 => V(\mathbf{w}) > 0$$

If $V(0) = 0$ and the above property holds over the whole state space, then $V(\mathbf{w})$ is said to be globally positive definite.

Definition A.7. *If, in a ball B_R , the function $V(\mathbf{w})$ is positive definite and has continuous partial derivatives, and if its time derivative along any state trajectory of system $\dot{\mathbf{w}} = \mathbf{f}(\mathbf{w})$ is negative semi-definite, i.e.,*

$$\dot{V}(\mathbf{w}) \leq 0$$

then $V(\mathbf{w})$ is said to be a Lyapunov function for the system $\dot{\mathbf{w}} = \mathbf{f}(\mathbf{w})$.

Theorem A.8. *If, in a ball B_R , there exists a scalar function $V(\mathbf{w})$ with continuous first partial derivatives such that*

- *$V(\mathbf{w})$ is positive definite (locally in B_R)*
- *$\dot{V}(\mathbf{w})$ is negative semi-definite (locally in B_R)*

then the equilibrium point $\mathbf{w}^*$ *is stable. If, actually, the derivative* $\dot{V}(\mathbf{w})$ *is locally negative definite in* B_R *, then the stability is asymptotic.*

Theorem A.9. *Assume that there exists a scalar function* $V(\mathbf{w}$*, with continuous first order derivatives such that*

- $V(\mathbf{w}$ *is positive definite*
- $\dot{V}(\mathbf{w}$ *is negative definite*
- $V(\mathbf{w} \to \infty$ *as* $||\mathbf{w}|| \to \infty$

then the equilibrium is globally asymptotically stable.

APPENDIX B: DEFINITIONS OF SYNCHRONIZATION

Synchronization of two dynamic systems has different definitions that depend on which features of the coupled systems are adjusted and how this happens.

- *Complete synchronization* (CS) (or *identical synchronization*) term is used for the synchronization of all state variables and phase of the oscillators in the network [36, 48]. For the coupled systems of the form given in Equation 2.13, *CS* is achieved, if Equation B.1 is satisfied.

$$\lim_{t\to\infty} \|\mathbf{w}_1(t) - \mathbf{w}_2(t)\| = \mathbf{0} \tag{B.1}$$

  $\mathbf{w}_1(t) = \mathbf{w}_2(t)$ is the *synchronization manifold* where the synchronous behavior converges in the long run. Stability on the *synchronization manifold* determines the ability to synchronize. In this thesis, the particular type of synchronization that will be considered is *CS*.

- *Projective synchronization* (*PrS*) is used if the states of the coupled systems are proportional to each other [60]. For the coupled systems given in Equation 2.13, *PrS* is achieved, if

$$\lim_{t\to\infty} \|\mathbf{w}_1(t) - \psi\mathbf{w}_2(t)\| = \mathbf{0} \tag{B.2}$$

  where ψ is a constant scalar. If $\boldsymbol{\psi} = diag[\psi_1, \psi_2, \ldots, \psi_N]$, then it is called *modified projective synchronization* (*MPrS*) [61]. If ψ is a function of time, $\psi(t)$, where $\psi(t)$ is continuously differentiable and $\psi(t) \neq 0$, then it is called *function projective synchronization* (*FPrS*) [62]. Another modification of *FPrS* which replaces $\boldsymbol{\psi}(t) = diag[\psi_1(t), \psi_2(t), \ldots, \psi_N(t)]$ where $\psi_i(t)$ is continuously differentiable and $\psi_i(t) \neq 0$, is called *modified function projective synchronization MFPrS* [63]. *CS* is a special form of *PrS* where $\psi = 1$, *MPrS* where $\boldsymbol{\psi} = I$, *FPrS* where $\psi(t) = 1 \quad \forall t$ and *MFPrS* where $\boldsymbol{\psi}(t) = I \quad \forall t$.

- *Generalized synchronization* (*GS*), as its name indicates, is a generalization of *PrS* and *CS*, which defines the synchronization condition as the difference between the state of one of the oscillators and a function of the state of the other oscillator tends to zero [40, 64]. *GS* is achieved if there exist a transformation $\mathbf{\Phi}$ from $\mathbf{W_1} \to \mathbf{W_2}$ and

$$\lim_{t\to\infty} \|\mathbf{w}_1(t) - \mathbf{\Phi}(\mathbf{w}_2(t))\| = \mathbf{0} \tag{B.3}$$

  where the mapping $\mathbf{\Phi}$ is considered only for the steady state of the trajectories on the strange attractor but not for the transient trajectories. Since *CS* is possible only for identical systems, *GS* can be extended to synchronization of nonidentical systems. In [40, 64], *GS* is shown for unidirectional coupling configuration. *GS* for network of mutually coupled oscillators is investigated in [65].

- *Phase synchronization* (*PhS*) refers to the case that phases of the oscillators are aligned however the amplitudes are unrelated [41]. *PhS* can also be extended to synchronization of nonidentical systems.

- *Lag synchronization* (*LS*) refers to synchronization with a shift in time [66]. For the coupled systems given in Equation 2.13, LS is achieved if

$$\lim_{t\to\infty} \|\mathbf{w}_1(t-\tau) - \mathbf{w}_2(t)\| = \mathbf{0} \tag{B.4}$$

  where τ represents the constant shift in time. LS is investigated for time-delayed systems in [67], for complex networks in [68]. In [69], *LS* is combined with *PrS* and *projective lag synchronization* (*PrLS*) is defined as:

$$\lim_{t\to\infty} \|\mathbf{w}_1(t-\tau) - \psi\mathbf{w}_2(t)\| = \mathbf{0} \tag{B.5}$$

  where ψ is a constant scalar.

APPENDIX C: CS-OGY ALGORITHM

The general algorithm for CS-OGY method proposed in this thesis is summarized in Figure C.1

Preparation

- Define a Poincaré surface S_p
- Choose the target UPO to be stabilized
- Determine heuristically a large enough region of linearizability around ζ^*
- Determine the range of the allowable perturbations on the control parameter.
- Obtain a local linear approximation of the Poincaré map around $\boldsymbol{\zeta} = \boldsymbol{\zeta}^*$ and $p = p_{nom}$
- Design a linear feedback control to stabilize linearized Poincaré map

for $t = T_{init}$ to T_{final} **do**

Run system until Poincaré surface S_p

Calculate $\Delta p_{calculated}$ for every T^{th} piercing (T is period of the UPO)

Saturate $\Delta p_{calculated}$. $\Delta p = saturate(\Delta p_{calculated})$

Apply Δp to the system

end for

Figure C.1. CS-OGY Control Algorithm.

APPENDIX D: PROOF OF THE STABILITY OF THE SYNCHRONIZATION OF BI-DIR-AD MEAN-FIELD COUPLED LORENZ SYSTEMS

Proof. Bidirectionally mean-field coupled Lorenz systems are:

$$\begin{aligned} \dot{x}_1 &= \sigma(y_1 - x_1) & \qquad \dot{x}_2 &= \sigma(y_2 - x_2) \\ \dot{y}_1 &= \rho\bar{x} - y_1 - \bar{x}z_1 & \qquad \dot{y}_2 &= \rho\bar{x} - y_2 - \bar{x}z_2 \\ \dot{z}_1 &= \bar{x}y_1 - \beta z_1 & \qquad \dot{z}_2 &= \bar{x}y_2 - \beta z_2 \end{aligned}$$

where $\bar{x} = \frac{x_1+x_2}{2}$. The error terms can be rewritten as;

$$\begin{aligned} e_x &= x_1 - x_2 \\ e_y &= y_1 - y_2 \\ e_z &= z_1 - z_2 \end{aligned}$$

and the error dynamics become;

$$\begin{aligned} \dot{e}_x &= \dot{x}_1 - \dot{x}_2 = \sigma(e_y - e_x) \\ \dot{e}_y &= \dot{y}_1 - \dot{y}_2 = -e_y - \bar{x}e_z \\ \dot{e}_z &= \dot{z}_1 - \dot{x}_2 = \bar{e}_{y1} - \beta e_z \end{aligned}$$

Let us define a Lyapunov function $V(e_x, e_y, e_z)$ as;

$$V(e_x, e_y, e_z) = \frac{1}{2}(\frac{1}{\sigma}e_x^2 + e_y^2 + e_z^2)$$

Derivative of $V(e_x, e_y, e_z)$ leads to;

$$\begin{aligned}
\dot{V}(e_x, e_y, e_z) &= \frac{1}{\sigma}e_x\dot{e}_x + e_y\dot{e}_y + e_z\dot{e}_z \\
&= \frac{1}{\sigma}e_x\sigma(e_y - e_x) + e_y(-e_y - \bar{x}e_z) + e_z(\bar{x}e_y - e_z) \\
&= e_xe_y - e_x^2 - e_y^2 - \bar{x}e_ye_z) + \bar{x}e_ye_z - \beta e_z^2 \\
&= e_xe_y - e_x^2 - e_y^2 - \beta e_z^2 \\
&= -(e_x - \frac{1}{2}e_y)^2 - \frac{3}{4}e_y^2 - \beta e_z^2 < 0
\end{aligned}$$

Therefore, $\forall\beta > 0$ synchronization error dynamics is stable.

$$\lim_{t\to\infty} \mathbf{e} = \mathbf{0}$$

□

Hence, Lorenz systems coupled with mean field of their x components will be synchronized.